

1 **Positional and ontogenetic variation in vertebral centra morphology in five batoid species**

2

3 Kelsey C James<sup>1</sup> and Lisa J Natanson<sup>2</sup>

4

5 <sup>1</sup>Department of Fisheries, Animal and Veterinary Sciences. University of Rhode Island, Rhode  
6 Island 02881, USA

7 <sup>2</sup>National Marine Fisheries Service, Northeast Fisheries Science Center, NOAA, Narragansett,  
8 Rhode Island 02882, USA

9

10 Corresponding author: [Kelsey.James@noaa.gov](mailto:Kelsey.James@noaa.gov)

11 Current address: NOAA Fisheries 8901 La Jolla Shores Dr. La Jolla, CA 92037

12

13 Running head: Morphology of batoid vertebral columns

14

15 **Abstract**

16 An increasing number of studies on elasmobranchs have shown that band pair counts in vertebral  
17 centra do not accurately reflect age. Research in sharks indicates that the number of band pairs  
18 vary with body size and centrum morphology is related to structural needs. A study of this kind  
19 has not been undertaken on batoids, thus we examined the relationship between band pair  
20 deposition and morphology of centra along the vertebral column, and ontogenetically, for five  
21 batoid species (little skate, *Leucoraja erinacea*, winter skate, *Leucoraja ocellata*, barndoor skate,  
22 *Dipturus laevis*, Atlantic stingray, *Dasyatis sabina*, and round ray, *Urobatis halleri*). Centrum  
23 morphology and band pair count varied along the vertebral column in all individuals of all  
24 species except in young of the year. Variation in band pair counts among centra within  
25 individuals supports the hypothesis that band pair formation is related to somatic growth and  
26 body shape rather than to an annual cycle.

27

28 Additional keywords: band pair counts, skates and rays, somatic growth, age

29

30

31 **Introduction**

32 The vertebral centra of elasmobranchs have characteristic alternating opaque and  
33 translucent bands (termed a band pair) that have been assumed to represent one year of growth  
34 and used to estimate age (Ridewood 1921; Haskell 1948; Ishiyama 1951; Cailliet *et al.* 2006).  
35 Annual band pair formation was assumed because more band pairs were found in the centra of  
36 larger individuals (Ridewood 1921). Subsequent studies demonstrated positive relationships  
37 between increasing body size and both centrum size and number of band pairs across individuals

38 (Ishiyama 1951; Jones and Geen 1977; Cailliet and Goldman 2004) supporting the use of  
39 vertebral bands pairs for age estimates.

40 Over time issues have become apparent in the use of vertebral band pairs for age estimates.  
41 Several species do not deposit band pairs annually, instead, depositing them relative to somatic  
42 growth (Natanson and Cailliet 1990; Tanaka 1990; Natanson *et al.* 2008). Other studies  
43 demonstrate decreased band pair deposition in older and larger individuals showing band pair  
44 counts underestimate age (see review by Harry 2018). Identifying these instances is critical to  
45 avoid inaccurate age estimates.

46 Another issue relates to the positive relationship between the number of band pairs and the  
47 size of the centrum. This positive relationship is true among individuals where larger individuals  
48 have larger centra with more band pairs (Cailliet and Goldman 2004), but it is also true within an  
49 individual; where centrum size and number of band pairs varies along the vertebral column  
50 (Natanson *et al.* 2018). Several studies have shown that small (young of the year [YOY])  
51 individuals often have the same number of band pairs throughout their vertebral column and  
52 similar centrum sizes however, band pair counts and centra size increasingly vary along the  
53 vertebral column in larger, maturing individuals of the same species (Natanson and Cailliet 1990;  
54 Natanson *et al.* 2008; Huveneers *et al.* 2013; Natanson *et al.* 2018). This has been shown in  
55 several species belonging to different families. If band pair deposition varies along the vertebral  
56 column with centrum size then band pair count cannot be related to age. Natanson *et al.* (2018)  
57 concluded that the number of band pairs vary along the column in direct correlation with the  
58 girth of the fish where the centra were taken and any relationship with time is not causative, but  
59 correlative through the somatic growth rate.

60 A majority of the research on elasmobranch vertebral column morphology and frequency  
61 of band pair deposition have been conducted on sharks, not batoids (Harry 2018; Natanson *et al.*  
62 2018). Ageing of batoids is subject to the same assumptions (Ishiyama 1951; Cailliet *et al.*  
63 2006), but there are only three confirmed batoid species demonstrating age underestimation  
64 (Natanson 1993; McPhie and Campana 2009; Pierce and Bennett 2009; James 2020). This is  
65 likely due to fewer validation studies on batoids (Harry 2018) rather than the absence of age  
66 underestimation.

67 The goal of the present study was to investigate whether vertebral band pairs are related  
68 to somatic growth and/or ontogeny in batoids. We measured centrum dimensions and counted  
69 the band pairs in individual centra along the columns of various-sized individuals of five batoid  
70 species (little skate, *Leucoraja erinacea*, winter skate, *Leucoraja ocellata*, barndoor skate,  
71 *Dipturus laevis*, Atlantic stingray, *Dasyatis sabina*, and round ray, *Urobotis helleri*; James  
72 2018). We then related centrum morphology to the number of band pairs of each centrum along  
73 the vertebral column and examined these relationships by size, sex, and species. Variation of  
74 band pair counts along the vertebral column of an individual calls into question the assumption  
75 that band pair formation is directly related to time, and raises concerns for using band pair counts  
76 for age estimates.

77

## 78 **Methods**

79 Skates were obtained opportunistically from commercial fishermen off the coast of  
80 Rhode Island and Massachusetts, USA. Atlantic stingrays were obtained from Seal Beach,  
81 California, and round rays from Indian River, Florida. Total length (TL; straight-line distance  
82 from snout tip to tail tip), and disc width (DW; straight-line distance from wing tip to wing tip)

83 were measured to the nearest 0.1 cm on all individuals. By convention, TL is used in analyses for  
84 skates, while DW is used in analyses for stingrays (Francis 2006). Sex and maturity status were  
85 determined by visually inspecting gonad condition (Ebert 2005).

86 Forty-two little skates (14 immature [small], 15 near size-at-maturity [medium], and 13  
87 mature [large]), six winter skates and six barndoor skates (two small, two medium, and two large  
88 of each), nine Atlantic stingrays (three small, three medium, and three large), and ten round rays  
89 (two small, four medium, and four large) were collected and measured for analysis of centrum  
90 morphology (Table 1; James 2018). Band pair counts were conducted along the vertebral  
91 columns of a subset of nine little skates, and six each of Atlantic stingray and round rays (Table  
92 1). The subset for each species included small, medium, and large individuals. All winter skates  
93 and barndoor skates were analyzed for the number of band pairs (Table 1). Males and females  
94 were evenly represented where possible (Table 1).

95

### 96 *Centrum Morphology*

97 The vertebral column was extracted from each fish starting with the first vertebra behind  
98 the synarcual cartilage and ending at the 80<sup>th</sup> vertebra. One round ray had sustained a tail injury  
99 and vertebrae were only available to the 48<sup>th</sup> centrum.

100 Each vertebral centrum was measured to the nearest 0.1 mm in three dimensions: dorso-  
101 ventral diameter (DVD), lateral diameter (LD) and rostro-caudal length (LEN), using Vernier  
102 calipers following Natanson *et al.* (2018) (Figure 1). Each measurement was divided by TL for  
103 the skate species and DW for the stingray species to standardize data across sizes for direct  
104 comparison. Standardized data were plotted against centrum number for each individual, noting  
105 the centrum number at the transition from abdominal cavity to tail.

106 Multiple generalized additive models (GAMs) were fit to each species using mgcv  
107 package in R (Wood 2011; R Core Team 2017) to assess whether each centrum measurement  
108 (DVD, LD, and LEN) was similar within a species, by sex, by size, or by individual (James  
109 2018). Four GAM variations were run for each measurement for each species: all data pooled,  
110 data grouped by sex, size class, and individual. Three GAM iterations were run: different  
111 intercepts only, different smoothing functions only, and different intercepts and smoothing  
112 functions for each sex, size class, and individual scenario. For each GAM variation the number  
113 of knots was specified to be larger than the estimated degrees of freedom using the gam.check  
114 function of mgcv in R. Model fit was assessed with Akaike's Information Criterion (AIC)  
115 (Haddon 2001).

116

#### 117 *Band Pair Counts*

118 To determine if band pair number varied along the vertebral column of an individual,  
119 every fifth centrum was processed histologically to visually enhance the band pairs (as per  
120 Natanson *et al.* 2007). Centrum sections were viewed under a dissecting microscope (Nikon  
121 SMZ1500<sup>®</sup>, Melville, NY, USA<sup>1</sup>) using reflected light and images were captured with a digital  
122 camera (Nikon DSR12, Tokyo, Japan) and image processing software (NIS Elements, v. 4.40,  
123 Nikon, Tokyo, Japan). Two band pair counts were made for each individual by a primary (KCJ)  
124 and a secondary reader using editing software (Adobe Photoshop CC (Adobe Systems, San Jose,  
125 CA, USA)). The birth band was identified as the first fully-formed band beyond the focus and  
126 was associated with an angle change in the corpus calcareum of the centrum (Casey *et al.* 1985;  
127 Cailliet and Goldman 2004). Each sample was assigned a unique ID number so that the reader

---

<sup>1</sup> Use of Trade Names does not imply endorsement from the NMFS.

128 had no knowledge of the size, sex, or location along the vertebral column. Coefficient of  
129 variation (CV) was calculated within and between readers to assess repeatability of counts and  
130 precision (Chang 1982). Values <10% were considered acceptable. Bias, as a result of either  
131 systematic or random error, was assessed using the Evans-Hoenig's (1998) test of symmetry.  
132 Band pair counts of zero are excluded from precision and bias analyses. Intra-reader precision  
133 and bias were compared between the first and second count of each reader while inter-reader  
134 precision and bias was compared between the second band pair counts. If the second band pair  
135 count differed by three or more band pairs, the centrum was examined together and a consensus  
136 count was reached. Final band pair counts were assigned from the primary reader's second count  
137 or the consensus count.

138 Final band pair count was plotted by centrum number for each individual. The mean band  
139 pair count and 95% confidence interval (CI) of the mean was calculated for each individual to  
140 test if band-pair count varied significantly among centra along the vertebral column. If more than  
141 5% of the band pair counts fell outside of the 95% CI then band pair counts were significantly  
142 different within an individual. A mixed-effects model was used to determine if there was a  
143 correlation between band pair count and the three centrum measurements for each species with  
144 individual included as a random effect.

145

## 146 **Results**

### 147 *Centrum Morphology*

148 Centrum morphology varied along the vertebral column in all species (Figure 2-6; James  
149 2018). The transition between abdominal and caudal centra occurred at the 24<sup>th</sup> to the 47<sup>th</sup>  
150 centrum depending on the species (Table 1). For little and winter skates DVD and LD increased

151 from the head and peaked at the level of the mid-abdominal cavity (approximately in line with  
152 the pectoral fin tips) then decreased through the transition from abdominal to caudal centra and  
153 continued to decrease in the caudal centra (Figures 2 and 3). Abdominal centra were wider than  
154 they were tall ( $LD > DVD$ ; ovoid), while caudal centra were circular ( $LD = DVD$ ; Figures 2 and  
155 3). Rostro-caudal length in little and winter skates increased from the head to the transition from  
156 abdominal to caudal centra where the LEN decreased sharply; LEN was constant among the  
157 caudal centra (Figures 2 and 3).

158         While trends in size of DVD and LD along the vertebral column in the barndoor skate  
159 were similar as in winter and little skates, the centra shape was different along the column.  
160 Barndoor skate centra were circular along the entire length of the column (Figure 4). In the  
161 barndoor skate, LEN followed a similar trend as in little and winter skates until approximately  
162 the 45<sup>th</sup> centrum, where LEN was greater than DVD and LD (Figure 4).

163         Atlantic stingray and round ray had similar centra morphologies, which differed from the  
164 skate species. In the rays, DVD and LD increased from the head, were constant along the  
165 abdominal cavity, and decreased in the caudal centra (Figures 5 and 6). Atlantic stingray and  
166 round ray centra were slightly ovoid along the abdominal cavity. Rostro-caudal length increased  
167 from the head until the transition from abdominal to caudal vertebrae after which LEN quickly  
168 decreased, but the decrease was less dramatic than that seen in the skate species. In both ray  
169 species, LEN was constant along the tail.

170         For all species studied, the centrum morphology along the vertebral column was best  
171 described by individual variation (Figure 7). The best-fit GAMs modeled each individual with its  
172 own intercept and smoothing function for all species and measurements rather than by sex or  
173 species (Supplemental Table 1; James 2018). The only exception was the LEN measurements in



174 Atlantic stingrays, which was best modeled by each individual with its own intercept, but the  
175 same smoothing function for all individuals (Supplemental Table 1). However, all models  
176 applied to the DVD and LD measurements of little skate, winter skate, barndoor skate, and round  
177 ray fit the data well with adjusted  $r^2 > 0.79$  (Supplemental Table 1). The LEN measurement for  
178 these species and all measurements for Atlantic stingray had lower adjusted  $r^2$  values ranging  
179 from 0.28 to 0.91 (Supplemental Table 1).

180

### 181 *Band Pair Counts*

182 The number of centra counted per batoid ranged from 11-17 (Table 1). Intra-reader CV  
183 ranged between 6.9 - 14.9% for primary reader and 6.4 - 12.5% for the secondary reader (Table  
184 2), while the inter-reader CV ranged from 10.1 - 21.4% (Table 2) depending on species. Of 478  
185 samples, 13.6% were read by consensus (Table 2). Intra-reader bias was detected for barndoor  
186 skate (primary reader) and for Atlantic stingray (secondary reader) using the Evans-Hoenig  
187 (1998) test of symmetry. Inter-reader bias was detected only for barndoor skate (Table 2).

188 Significant differences in band pair counts were found along the column of all individuals  
189 except in YOY. Excluding YOY, 17.6 – 100% of the band pair counts fell outside of the 95% CI  
190 (Figures 2-6; James 2018). The band pair counts for the three skate species were roughly  
191 correlated with the pattern of the DVD and LD measurements (Figures 2-4). Band pair counts for  
192 the Atlantic stingray and the round ray did not exhibit a trend along the vertebral column, but  
193 still showed significant differences among different centra within an individual (Figures 5 and 6).  
194 The largest range in band pair counts within an individual was seven band pairs for little skate,  
195 eight band pairs for winter skate, 11 band pairs in barndoor skate, five band pairs in Atlantic  
196 stingray, and six band pairs for round ray. Abdominal centra typically had higher band pair

197 counts than caudal centra. The two smallest Atlantic stingray specimens examined were YOY  
198 and did not have band pairs (Figure 5).

199         The number of band pairs was related to centrum morphology in all species, except  
200 winter skate. Dorso-ventral diameter, LD, and LEN were significantly correlated with the band  
201 pair counts of little skate, barndoor skate, and round ray (Table 3; James 2018). Atlantic stingray  
202 were significantly correlated with DVD and LD, but not with LEN. Winter skate did not have  
203 any significant correlations.

204

## 205 **Discussion**

206         Variable band pair counts among centra within an individual has now been observed in  
207 15 species representing 9 elasmobranch families (Natanson and Cailliet 1990; Natanson *et al.*  
208 2008; Huveneers *et al.* 2013; Natanson *et al.* 2018; current study). The presence of this variation  
209 suggests that the mechanism that regulates the formation of band pairs is not related to time.  
210 When differences in band pair counts between more anterior and more posterior centra were  
211 detected in previous studies, it was suggested that band pairs in smaller, caudal centra were more  
212 difficult to interpret (Brown and Gruber 1988; Officer *et al.* 1996; Natanson *et al.* 2006; Piercy *et*  
213 *al.* 2006). In this study we did not find it difficult to interpret band pairs in smaller centra, and we  
214 confirmed that the number of band pairs within an individual varies along the vertebral column  
215 in batoids. Band pair counts that vary among centra along the vertebral column of an individual  
216 cannot accurately reflect a single age estimate (Natanson *et al.* 2018). The positive relationship  
217 observed between band pair count and centra morphology for four of the five batoid species  
218 examined in this study makes band pair counts unreliable as a tool for ageing in these species.

219           The hypothesis that structural needs of the individual may regulate the formation of band  
220 pairs is suggested on the basis that mineralization of the centra enhances skeletal strength and  
221 mechanical support (Kemp and Westrin 1979; Clement 1992; Porter *et al.* 2006; 2007).  
222 Regardless of species, larger centra have more band pairs indicating that band pair deposition is a  
223 structural requirement of the individual and not related to time (Natanson *et al.* 2018). The  
224 positive correlation of body girth measurements to centrum size led Natanson *et al.* (2018) to  
225 suggest that differences in deposition patterns are correlated with body type and swimming mode  
226 among species. This was supported by Thomson and Simanek's (1977) five categories of body  
227 and tail type, in which species of similar body shapes and swimming styles also had similar  
228 centrum morphology and Ingle *et al.* (2018) who found that larger centra with more band pairs  
229 had lower toughness and stiffness than smaller centra with fewer band pairs. More band pairs  
230 (present in abdominal vertebrae) may support body mass, while fewer band pairs (present in  
231 anterior and posterior vertebrae) with higher toughness and stiffness allow absorption of more  
232 energy and elastic recoil to facilitate swimming (Ingle *et al.* 2018; Natanson *et al.* 2018). Batoids  
233 possess vastly different swimming styles than many sharks, however the Atlantic angel shark  
234 uses a swimming mode that is an intermediate between caudal fin propulsion and paired fin  
235 propulsion (Wilga and Lauder 2004). These dorso-ventrally flattened sharks also demonstrate a  
236 relationship between body shape and centrum morphology (Natanson *et al.* 2018), so it is  
237 reasonable to extend this relationship to batoids. The body girth measurements used by Natanson  
238 *et al.* (2018) did not translate to a batoid body plan (James, unpub. data) so a different approach  
239 will have to be used to investigate the relationship between body shape and centrum  
240 morphology.

241 Centrum morphologies in these five batoid species were roughly similar to the centrum  
242 morphology of sharks (Natanson *et al.* 2018). The Atlantic angel shark had the most similar  
243 centrum morphology to the batoids with the largest centrum in the middle of the abdominal  
244 cavity (approximately in line with the tips of the pectoral fins), while the largest centrum for the  
245 other shark species was at the end of the abdominal cavity (Natanson *et al.* 2018). The Atlantic  
246 angel shark also had ovoid centra (Natanson *et al.* 2018) similar to the abdominal centra of  
247 batoids. In carcharhinids and lamnids, centra were circular, except for the abdominal centra of  
248 very large lamnids (i.e. shortfin mako; Natanson *et al.* 2018). We suggest that ovoid centra are  
249 characteristic of dorso-ventrally compressed elasmobranchs and may be related to undulation of  
250 pectoral fins as a swimming strategy, a benthic lifestyle, or the ability to bend dorso-ventrally,  
251 not just laterally as in most sharks.

252 Similarities in centrum morphology exist across and within species. Individual variation  
253 was the best descriptor of centrum morphology for batoids, however most GAMs fit the data  
254 well (Supplemental Table 1). The good fit of these models may be in part due to the uniformity  
255 of morphology of caudal vertebrae (e.g. Figure 7). In contrast, abdominal vertebrae display high  
256 individual variation (e.g. Figure 7) suggesting that the conditions an individual experiences  
257 influences growth. In Atlantic salmon, *Salmo salar* Linnaeus 1758, centra within an individual  
258 grew at different rates depending on the photoperiod regime (Fjellidal *et al.* 2005). Based on our  
259 results, we suggest that factors affecting individual body growth (food availability, temperature,  
260 population density, and genetics [McDowall 1994]) may also affect individual centrum  
261 morphology in batoids.

262 The paradigm of annual band pair deposition within centra of elasmobranchs has been  
263 disproven in many species (Natanson and Cailliet 1990; Tanaka 1990; Francis *et al.* 2007;

264 Huveneers *et al.* 2013; Harry 2018; Natanson *et al.* 2018). Here we add to that body of literature  
265 with five batoids species, supporting the idea that band pair number is related to somatic growth  
266 and/or the structural needs of the individual in elasmobranchs as a group (Natanson and Cailliet  
267 1990; Tanaka 1990; Natanson *et al.* 2008; Natanson *et al.* 2018). We also reinforce the call for  
268 caution when using band pair counts as a proxy of age without validation (Beamish and  
269 MacFarlane 1983). Future work investigating the impact of inaccurate ages on stock-assessment  
270 model results and determining an alternate method to age elasmobranchs should be at the  
271 forefront of elasmobranch ageing.

272

### 273 **Conflicts of Interest**

274 The authors declare no conflicts of interest.

275

### 276 **Acknowledgements**

277 We thank M. Winton for providing R code. We thank K. Lyons for donating specimens and  
278 being a secondary reader. We thank K. Fagan, K. Viducic, and K. Wooley for being secondary  
279 readers. We thank R. Skyes, the crew of the F/V *Virginia Marise*, the crew of the R/V *Cap'n*  
280 *Bert*, the Cape Cod Fishermen's Alliance, and D. Adams for collection assistance. We thank A.  
281 Tumminelli for data collection assistance. Collection of skates occurred under a Rhode Island  
282 Collector's Permit #2015-06 and #2016-51. Research was supported by the Marine Anglers for  
283 Research and Conservation Memorial, and an American Elasmobranch Society Student Research  
284 Award, and the University of Rhode Island. This paper forms part of the PhD thesis of Kelsey  
285 James (2018).

286 **References**

287 Beamish, R. J., and McFarlane, G. A. (1983). The forgotten requirement for age validation in  
288 fisheries biology. *Transactions of the American Fisheries Society* **112**, 735-743.

289

290 Brown, C. A., and Gruber, S. H. (1988). Age assessment of the Lemon shark, *Negaprion*  
291 *brevirostris*, using tetracycline validated vertebral centra. *Copeia* **1988**, 747-753.

292

293 Cailliet, G. M., and Goldman, K. J. (2004). Ch 14 Age determination and validation in  
294 Chondrichthyan fishes. *Biology of sharks and their relatives 2004* CRC Press LLC

295

296 Cailliet, G. M., Smith, W. D., Mollet, H. F., and Goldman, K. J. (2006). Age and growth studies  
297 of chondrichthyan fishes: the need for consistency in terminology, verification,  
298 validation, and growth function fitting. *Environmental Biology of Fishes* **77**, 211-228.

299

300 Casey, J. G., Pratt, H. L., and Stillwell, C. E. (1985). Age and growth of the sandbar shark  
301 (*Carcharhinus plumbeus*) from the Western North Atlantic. *Canadian Journal of*  
302 *Fisheries and Aquatic Sciences* **42**, 963-975.

303

304 Chang, W. Y. B. (1982). A statistical method for evaluating the reproducibility of age  
305 determination. *Canadian Journal of Fisheries and Aquatic Sciences* **39**, 1208-1210.

306

307 Clement, J. G. (1992). Re-examination of the fine structure of endoskeletal mineralization in  
308 Chondrichthyans: Implications for growth, ageing and calcium homeostasis. Australian  
309 Journal of Marine and Freshwater Research **43**, 157-181.

310

311 Ebert, D. A. (2005). Reproductive biology of skates, *Bathyraja* (Ishiyama), along the eastern  
312 Bering Sea continental slope. Journal of Fish Biology **66**, 618-649.

313

314 Evans, G. T., and Hoenig, J. M. (1998). Testing and viewing symmetry in contingency tables,  
315 with applications to readers of fish ages. Biometrics **54**, 620-629.

316

317 Fjellidal, P. G., Nordgarde, U., Berg, A., Grotmol, S., Totland, G. K., Wargelius, A., and Hansen,  
318 T. (2005). Vertebrae of the trunk and tail display different growth rates in response to  
319 photoperiod in Atlantic salmon, *Salmo salar* L., post-smolts. Aquaculture **250**, 516-524.

320

321 Francis, M.P. (2006). Morphometric minefields—towards a measurement standard for  
322 chondrichthyan fishes. Environmental Biology of Fishes **77**, 407-421.

323

324 Francis, M. P., Campana, S. E., and Jones, C. M. (2007). Age under-estimation in New Zealand  
325 Porbeagle Sharks (*Lamna nasus*): is there an upper limit to ages that can be determined  
326 from shark vertebrae? Marine and Freshwater Research **58**, 10-23.

327

328 Haddon, M. (2001). Modeling and quantitative measures in fisheries. Chapman & Hall/CRC  
329 Press, Boca Raton FL

330  
331  
332  
333  
334  
335  
336  
337  
338  
339  
340  
341  
342  
343  
344  
345  
346  
347  
348  
349  
350  
351  
352

Harry, A. V. (2018). Evidence of systemic age underestimation in shark and ray ageing studies. *Fish and Fisheries* **2018**, 1-16.

Haskell, W. L. (1948). An investigation of the possibility of determining the age of sharks through annuli as shown in cross-sections of vertebrae. Annual Report of the Marine Laboratory of the Texas Game, and Fish Commission **FY 1948-49**, 212-217.

Huveneers, C., Stead, J., Bennett, M. B., Lee, K. A., and Harcourt, R. G. (2013). Age and growth determination of three sympatric wobbegong sharks: How reliable is growth band periodicity in Orectolobidae? *Fisheries Research* **147**, 413-425.

Ingle, D. I., Natanson, L. J., and Porter, M. E. (2018). Mechanical behavior of shark vertebral centra at biologically relevant strains. *Journal of Experimental Biology* **221**, jeb188318.

Ishiyama, R. (1951). Studies on the rays and skates belonging to the family Rajidae, found in Japan and adjacent regions. 2. On the age-determination of Japanese Black-Skate *Raja fusca*. *Bulletin of the Japanese Society for the Science of Fish* **16**, 112-118.

James, K.C. (2018). Analysis of band pair formation in elasmobranch vertebrae with implications for fisheries management. PhD Thesis. University of Rhode Island. Open Access Dissertations. Paper 760.



353 James, K.C. (2020). Vertebral growth and band-pair deposition in sexually mature little skates  
354 *Leucoraja erinacea*: is adult band-pair deposition annual? Journal of Fish Biology **96**, 4-  
355 13.

356

357 Jones, B. C., and Geen, G. H. (1977). Age determination of an elasmobranch (*Squalus acanthias*)  
358 by x-ray spectrometry. Journal of the Fisheries Research Board of Canada **34**, 44-48.

359

360 Kemp, N. E., and Westrin, S. K. (1979). Ultrastructure of calcified cartilage in the endoskeletal  
361 tesserae of sharks. Journal of Morphology **160**, 75-102.

362

363 McDowall, R. M. (1994). On size and growth in freshwater fish. Ecology of Freshwater Fish **3**,  
364 67-79.

365

366 McPhie, R. P., and Campana, S. E. (2009). Bomb dating and age determination of skates (family  
367 Rajidae) off the eastern coast of Canada. ICES Journal of Marine Science **66**, 546-560.

368

369 Natanson, L. J. (1993). Effect of temperature on band deposition in the Little Skate, *Raja*  
370 *erinacea*. Copeia **1993**, 199-206.

371

372 Natanson, L., Kohler, N., Ardizzone, D., Cailliet, G., Wintner, S., and Mollet, S. (2006).  
373 Validated age and growth estimates for the shortfin mako, *Isurus oxyrinchus*, in the North  
374 Atlantic Ocean. Environmental Biology of Fishes **77**, 367-383.

375

376 Natanson, L. J., and Cailliet, G. M. (1990). Vertebral growth zone deposition in Pacific Angel  
377 Sharks. *Copeia* **1990**, 1133-1145.  
378

379 Natanson, L. J., Skomal, G. B., Hoffmann, S., Porter, M., Goldman, K. J., and Serra, D. (2018).  
380 Age and growth of elasmobranchs: do band pairs on vertebral centra record age? *Marine*  
381 *and Freshwater Research* **69**, 1440-1452.  
382

383 Natanson, L. J., Sulikowski, J. A., Kneebone, J. R., Tsang, P. C. (2007). Age and growth  
384 estimates for the Smooth Skate, *Malacoraja senta*, in the Gulf of Maine. *Environmental*  
385 *Biology of Fishes* **80**, 293-308.  
386

387 Natanson, L. J., Wintner, S., Johansson, F., Piercy, A. N., Campbell, P., De Maddalena, A.,  
388 Gulak, S. J., Human, B., Fulgosi, F. C., Ebert, D. A., Hemida, F., Mollen, F. H., Vanni,  
389 S., Burgess, G. H., Compagno, L. J. V., and Wedderburn-Maxwell, A. (2008).  
390 Ontogenetic vertebral growth patterns in the Basking Shark, *Cetorhinus maximus*. *Marine*  
391 *Ecology Progress Series* **361**, 267-278.  
392

393 Officer, R. A., Gason, A. S., Walker, T. I., and Clement, J. G. (1996). Sources of variation in  
394 counts of growth increments in vertebrae from gummy shark, *Mustelus antarcticus*, and  
395 school shark, *Galeorhinus galeus*: implications for age determination. *Canadian Journal*  
396 *of Fisheries and Aquatic Sciences* **53**, 1765-1777.  
397

398 Pierce, S. J., and Bennett, M. B. (2009). Validated annual band-pair periodicity and growth  
399 parameters of blue-spotted maskray *Neotrygon kuhlii* from south-east Queensland,  
400 Australia. *Journal of Fish Biology* **75**, 2490-2508.  
401

402 Piercy, A. N., Ford, T. S., Levy, L. M., and Snelson, F. F. (2006). Analysis of variability in  
403 vertebral morphology and growth ring counts in two Carcharhinid sharks. *Environmental*  
404 *Biology of Fishes* **77**, 401-406.  
405

406 Porter, M. E., Beltran, J. L., Koob, T. J., and Summers, A. P. (2006). Material properties and  
407 biochemical composition of mineralized vertebral cartilage in seven elasmobranch  
408 species (Chondrichthyes). *The Journal of Experimental Biology* **209**, 2920-2928.  
409

410 Porter, M. E., Koob, T. J., and Summers, A. P. (2007). The contribution of mineral to the  
411 material properties of vertebral cartilage from the smooth-hound shark *Mustelus*  
412 *californicus*. *The Journal of Experimental Biology* **210**, 3319-3327.  
413

414 R Core Team. (2017). R: A language and environment for statistical computing. R Foundation  
415 for Statistical Computing, Vienna, Austria URL <https://www.R-project.org/>.  
416

417 Ridewood, W. G. (1921). On the calcification of the vertebral centra in sharks and rays.  
418 *Philosophical Transactions of the Royal Society B* **210**, 311-407.  
419

420 Tanaka, S. (1990). Age and growth studies on the calcified structures of newborn sharks in  
421 laboratory aquaria using tetracycline. In *Elasmobranchs as Living Resources: Advances*  
422 *in the Biology, Ecology, Systematics, and the Status of Fisheries* NOAA Technical  
423 Report **90**, 189-202.

424

425 Thomson, K. S., and Simanek, D. E. (1977). Body form and locomotion in sharks. *American*  
426 *Zoologist* **17**, 343-354.

427

428 Wilga, C. A. D., and Lauder, G. V. (2004). Biomechanics of locomotion in sharks, rays, and  
429 chimeras. Carrier, J. C., Musick, J. A., and Heithaus, M. R. (*eds.*) *Biology of Sharks and*  
430 *Their Relatives* 2004 CRC Press LLC

431

432 Wood, S. N. (2011). Fast stable restricted maximum likelihood and marginal likelihood  
433 estimation of semiparametric generalized linear models. *Journal of the Royal Statistical*  
434 *Society B* **73**, 3-36.

435

436 **Table and Figure Captions**

437

438 Table 1. Individuals of five batoid species used in this study. For little skate *Leucoraja erinacea*,  
439 the first nine individuals were analyzed for band pair counts. For winter skate *Leucoraja*  
440 *ocellata*, barndoor skate *Dipturus laevis*, Atlantic stingray *Dasyatis sabina*, and round ray  
441 *Urobatis halleri*, the first six individuals were analyzed for band pair counts. All individuals  
442 were measured for centrum morphology. For brevity, only condensed data are presented for the  
443 additional 33 little skates used for centrum morphology. TL is total length, DW is disc width, L  
444 is large, M is medium in the Size column and Male in the Sex column, S is for small, F is for  
445 female.

446

447 Table 2. Bias and precision of band-pair counts within and between readers. Asterisk indicates  
448 significant bias.

449

450 Table 3. Linear mixed-effects model comparing band-pair counts with the three centrum  
451 measurements with individual included in the model as a random effect. Asterisk indicates  
452 significant correlation.

453

454 Figure 1. Diagram of a vertebral centrum and the three measurements: dorso-ventral diameter  
455 (DVD), lateral diameter (LD), and rostro-caudal length (LEN). R is rostral and C is caudal.

456

457 Figure 2. Band-pair count and standardized centrum measurements along the vertebral column  
458 for nine little skates analyzed for band pairs.

459

460 Figure 3. Band-pair count and standardized centrum measurements along the vertebral column  
461 for the six winter skates analyzed for band pairs.

462

463 Figure 4. Band-pair count and standardized centrum measurements along the vertebral column  
464 for six barndoor skates analyzed for band pairs.

465

466 Figure 5. Band-pair count and standardized centrum measurements along the vertebral column  
467 for six Atlantic stingrays analyzed for band pairs.

468

469 Figure 6. Band-pair count and standardized centrum measurements along the vertebral column  
470 for six round rays analyzed for band pairs.

471

472 Figure 7. Example of generalized additive model variations with (a) all data pooled, data pooled  
473 (b) by sex, (c) by size class, and (d) by individual fit to barndoor skate data.

474

475 Supplemental Table 1. Generalized additive model results for 10 different models to best  
476 describe centrum morphology along the vertebral column for five batoid species. k is the number  
477 of knots used in each model.

Table 1. Individuals of five batoid species used in this study. For little skate *Leucoraja erinacea*, the first nine individuals were analyzed for band pair counts. For winter skate *Leucoraja ocellata*, barndoor skate *Dipturus laevis*, Atlantic stingray *Dasyatis sabina*, and round ray *Urobatis halleri*, the first six individuals were analyzed for band pair counts. All individuals were measured for centrum morphology. For brevity, only condensed data are presented for the additional 33 little skates used for centrum morphology. TL is total length, DW is disc width, L is large, M is medium in the Size column and Male in the Sex column, S is for small, F is for female.

Species	TL (cm)	DW (cm)	Size	Sex	Maturity	Transition <sup>a</sup>	Centra Counted <sup>b</sup>	Individual ID
<b>Little Skate</b>	49.0	29.0	L	F	Mature	22	13	LE03
	48.5	29.5	L	M	Mature	22	12	LE01
	48.0	27.0	L	F	Mature	24	17	LE07
	42.8	25.2	M	F	Immature	27	17	LE06
	41.5	23.8	M	M	Mature	26	17	LE05
	39.6	24.0	M	F	Immature	27	17	LE19
	26.1	14.5	S	M	Immature	26	17	LE04
	25.6	15.5	S	F	Immature	21	14	LE02
	23.4	13.7	S	F	Immature	22	15	LE20
43.0-47.5	24.6-27.3	L	5 F, 5 M	1 Immature, 9 Mature	22-25	N/A	N/A	
38.3-42.4	22.8-25.4	M	5 F, 7 M	11 Immature, 2 Mature	23-26	N/A	N/A	
25.1-32.6	15.2-19.8	S	5 F, 6 M	Immature	21-25	N/A	N/A	
<b>Winter Skate</b>	80.0	49.9	L	F	Mature	27	17	LO04
	75.3	47.8	L	M	Mature	30	17	LO07
	63.3	39.1	M	F	Immature	26	17	LO08
	61.7	40.5	M	M	Immature	27	16	LO09
	43.2	26.9	S	M	Immature	31	17	LO06
	37.1	22.0	S	F	Immature	29	16	LO05
<b>Barndoor Skate</b>	130.0	92.6 <sup>c</sup>	L	M	Mature	25	17	DL04

	117.4	80.9	L	F	Mature	25	17	DL16
	107.5	76.7 <sup>c</sup>	M	F	Mature	27	14	DL01
	90.0	64.3 <sup>c</sup>	M	M	Immature	27	16	DL03
	52.3	37.6	S	F	Immature	31	17	DL05
	49.0	36.3	S	M	Immature	24	17	DL06
<b>Atlantic Stingray</b>	48.9	26.5	L	F	Mature		15	DS24
	44.8	26.9	L	F	Mature	36	17	DS26
	40.0	18.0	M	F	Immature	49	16	DS32
	36.6	17.8	M	F	Immature	46	17	DS30
	34.2	13.4	S	F	Immature	46	16	DS27
	25.0	13.3	S	F	Immature	47	15	DS33
	59.8	30.3	L	F	Mature	31	N/A	DS31
	42.6	16.0	M	F	Immature	46	N/A	DS29
	30.0	11.0	S	M	Immature	46	N/A	DS25
<b>Round Ray</b>	36.7	20.4	L	M	Mature	31	17	UH01
	21.3	20.0	L	F	Mature	32	11	UH08
	30.5	16.7	M	F	Mature	32	17	UH05
	30.0	16.5	M	M	Mature	34	16	UH10
	24.0	13.3	S	M	Immature	34	17	UH09
	22.8	13.1	S	F	Immature	41	17	UH07
	34.2	19.8	L	M	Mature	34	N/A	UH02
	33.4	18.6	L	M	Mature	30	N/A	UH03
	29.9	17.8	M	F	Mature	31	N/A	UH04
	27.2	16.1	M	F	Mature	31	N/A	UH06

<sup>a</sup>Vertebral number where the transition between abdominal and caudal vertebrae occurs.

<sup>b</sup>Number of centra counted for each individual. N/A means band-pair counts were not determined.

<sup>c</sup>Disc Width was estimated using Total Length to Disc Width relationship from Gedamke 2006.

Table 2. Bias and precision of band pair counts within and between readers for each of the five batoid species. n is the total number of centra counted.

Species		Evans-Hoenig (1998) Bias test					
		n <sup>a</sup>	df	$\chi^2$	p	CV	Consensus <sup>b</sup>
<b>Little Skate</b>	Primary reader		4	8.71	0.069	9.08	
	Second reader		3	2.38	0.497	11.89	
	Inter-reader	130	7	11.09	0.135	16.77	16
<b>Winter Skate</b>	Primary reader		6	11.30	0.800	6.86	
	Second reader		5	7.69	0.174	8.80	
	Inter-reader	99	6	7.22	0.301	10.08	11
<b>Barndoor Skate</b>	Primary reader		5	11.49	0.042	* 9.35	
	Second reader		4	3.42	0.490	6.37	
	Inter-reader	95	5	12.63	0.027	* 16.61	14
<b>Atlantic Stingray</b>	Primary reader		3	2.50	0.475	14.88	
	Second reader		2	9.76	0.008	* 12.54	
	Inter-reader	63	4	8.43	0.077	21.35	9
<b>Round Ray</b>	Primary reader		4	4.06	0.398	9.81	
	Second reader		3	2.44	0.486	9.93	
	Inter-reader	91	4	3.31	0.507	11.83	15

<sup>a</sup>Band pair counts of zero are excluded from bias and precision analyses

<sup>b</sup>Number of centra counted by both readers together for consensus.



Table 3. Linear mixed-effects model comparing band pair counts with the three centrum measurements with individual included the model as a random effect. Asterisk indicates significant correlation.

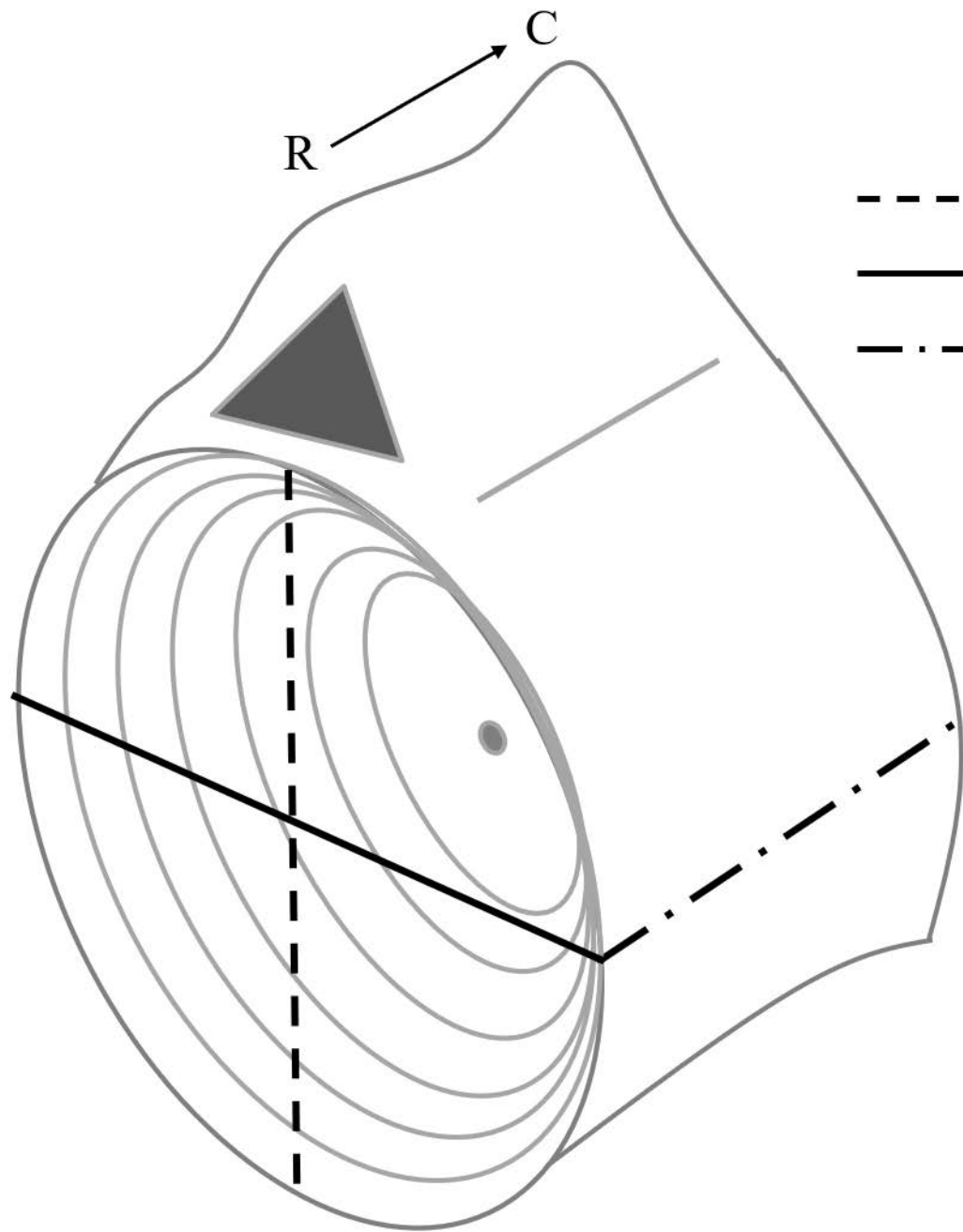
Species	Measurement	Estimate	S.E.	df	t-value	p-value	
Little Skate	Dorsal Diameter	0.591	0.218	129	2.716	0.0075	*
	Lateral Diameter	0.435	0.140	129	3.101	0.0024	*
	Length	0.624	0.300	127	2.078	0.0398	*
Winter Skate	Dorsal Diameter	0.123	0.184	93	0.667	0.5066	
	Lateral Diameter	0.092	0.146	93	0.628	0.5316	
	Length	-0.325	0.364	92	0.894	0.3737	
Barndoor Skate	Dorsal Diameter	0.572	0.148	91	3.864	0.0002	*
	Lateral Diameter	0.646	0.154	91	4.205	0.0001	*
	Length	0.666	0.244	90	2.732	0.0076	*
Atlantic Stingray	Dorsal Diameter	0.865	0.326	88	2.649	0.0096	*
	Lateral Diameter	0.961	0.210	88	4.574	0.0000	*
	Length	0.915	0.499	87	1.833	0.0703	
Round Ray	Dorsal Diameter	0.807	0.278	88	2.909	0.0046	*
	Lateral Diameter	0.625	0.264	88	2.371	0.0199	*
	Length	0.900	0.431	86	2.085	0.0400	*

R → C

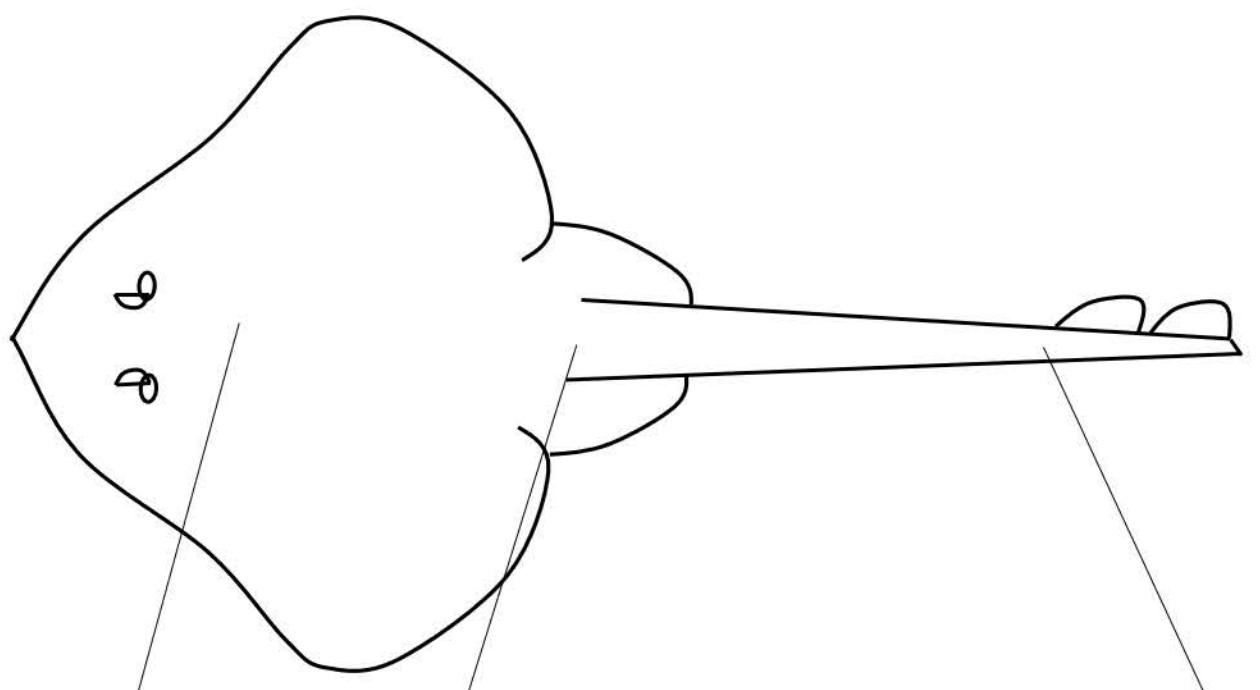
--- Dorso-ventral Diameter

— Lateral Diameter

- . - . Rostro-caudal Length

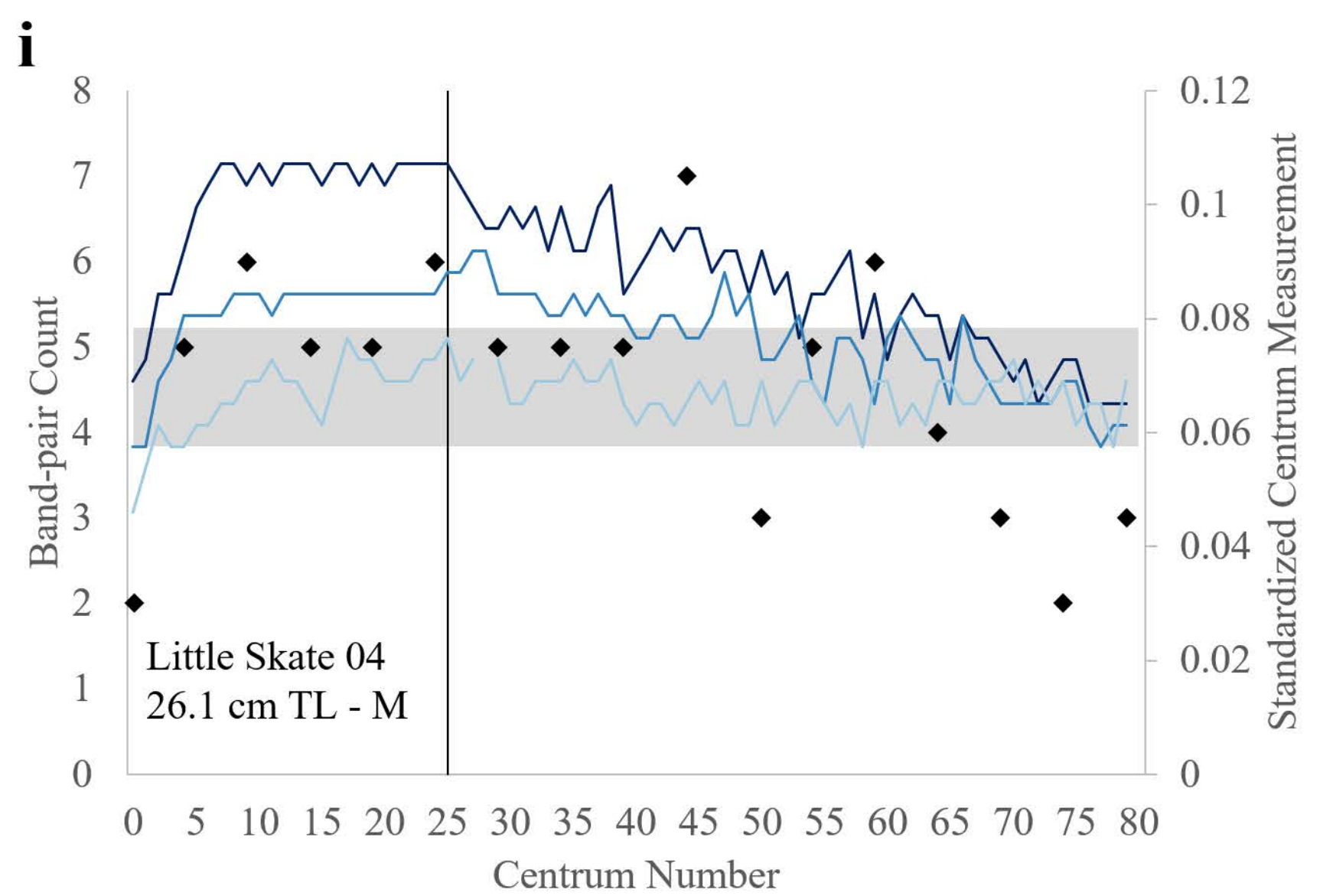
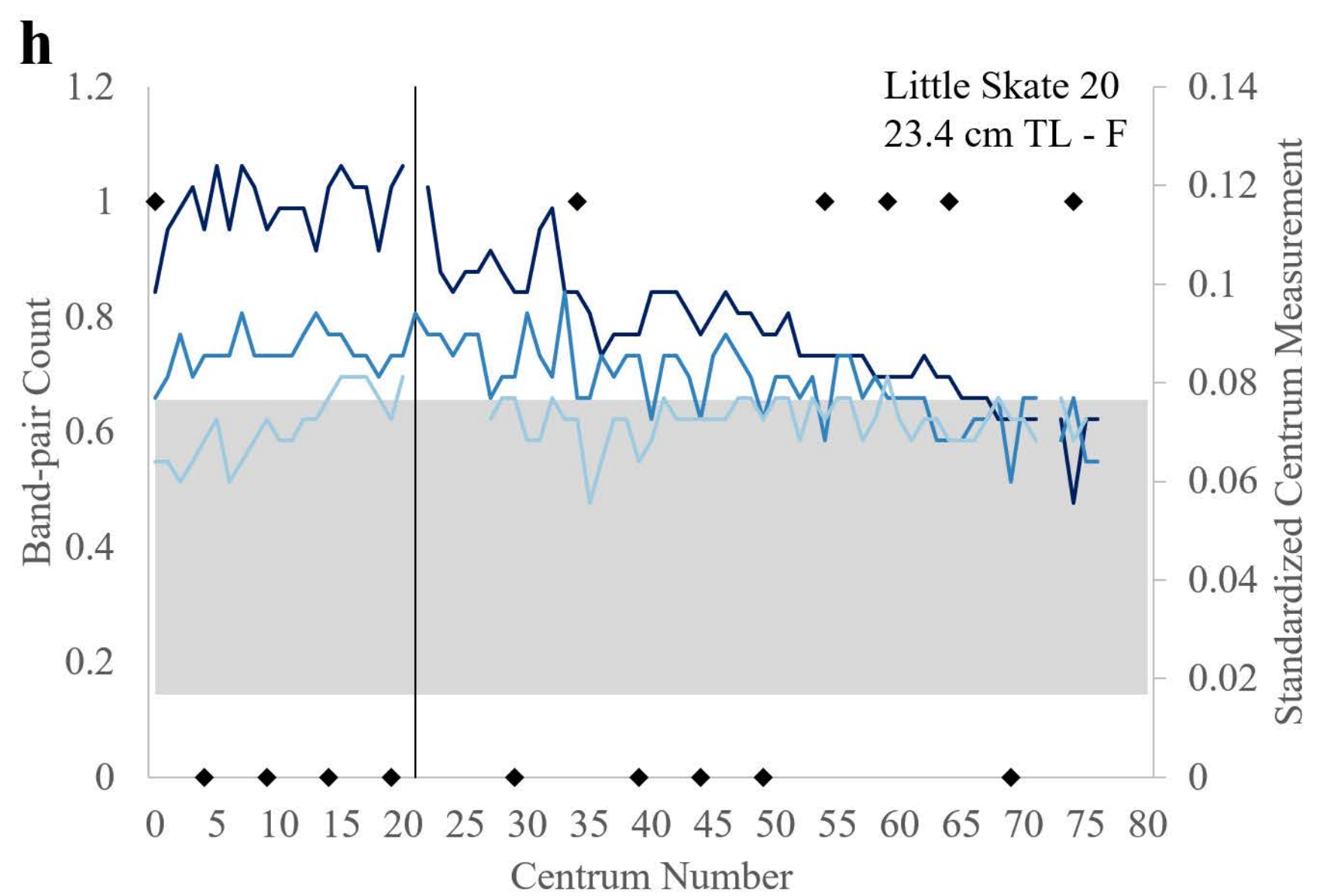
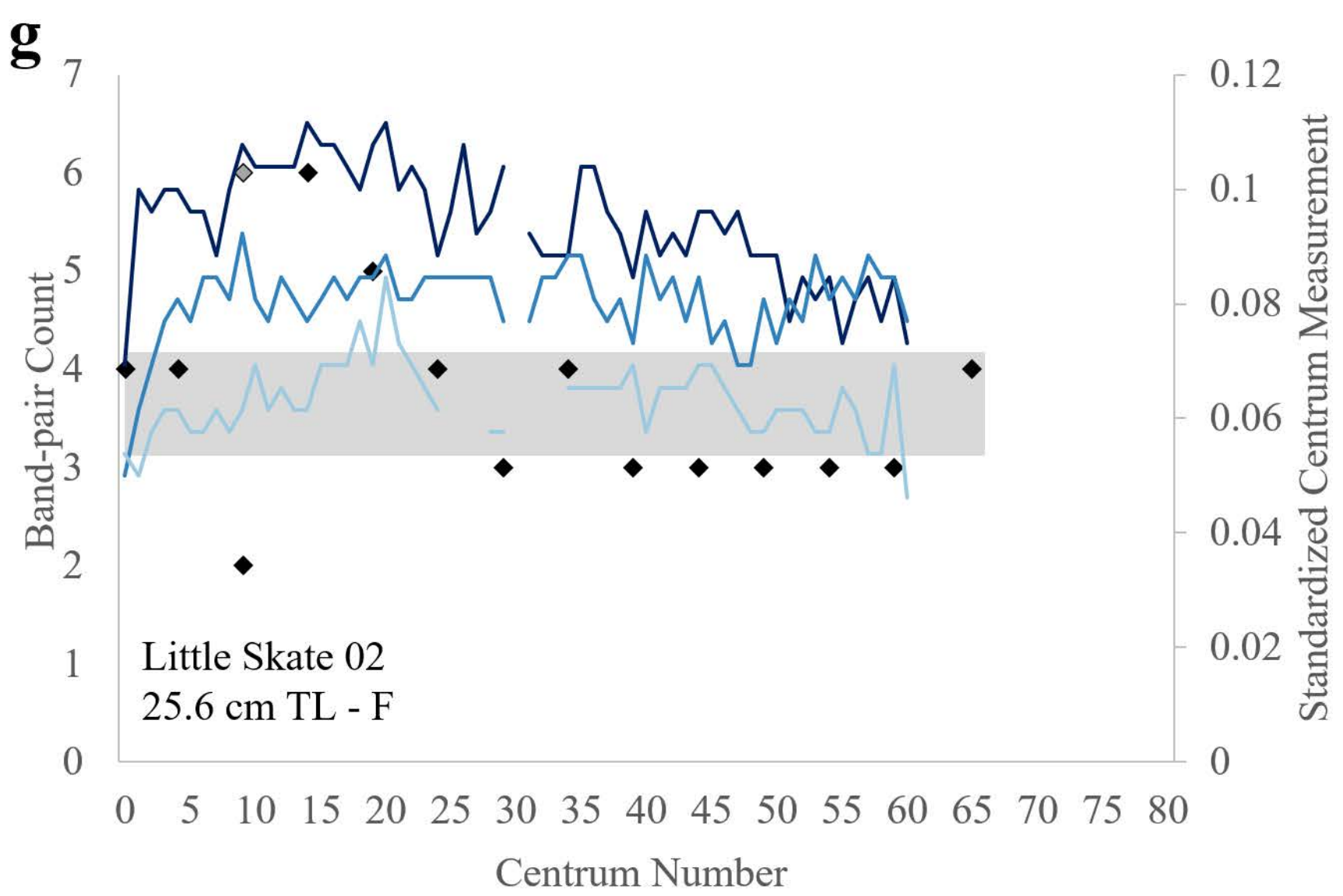
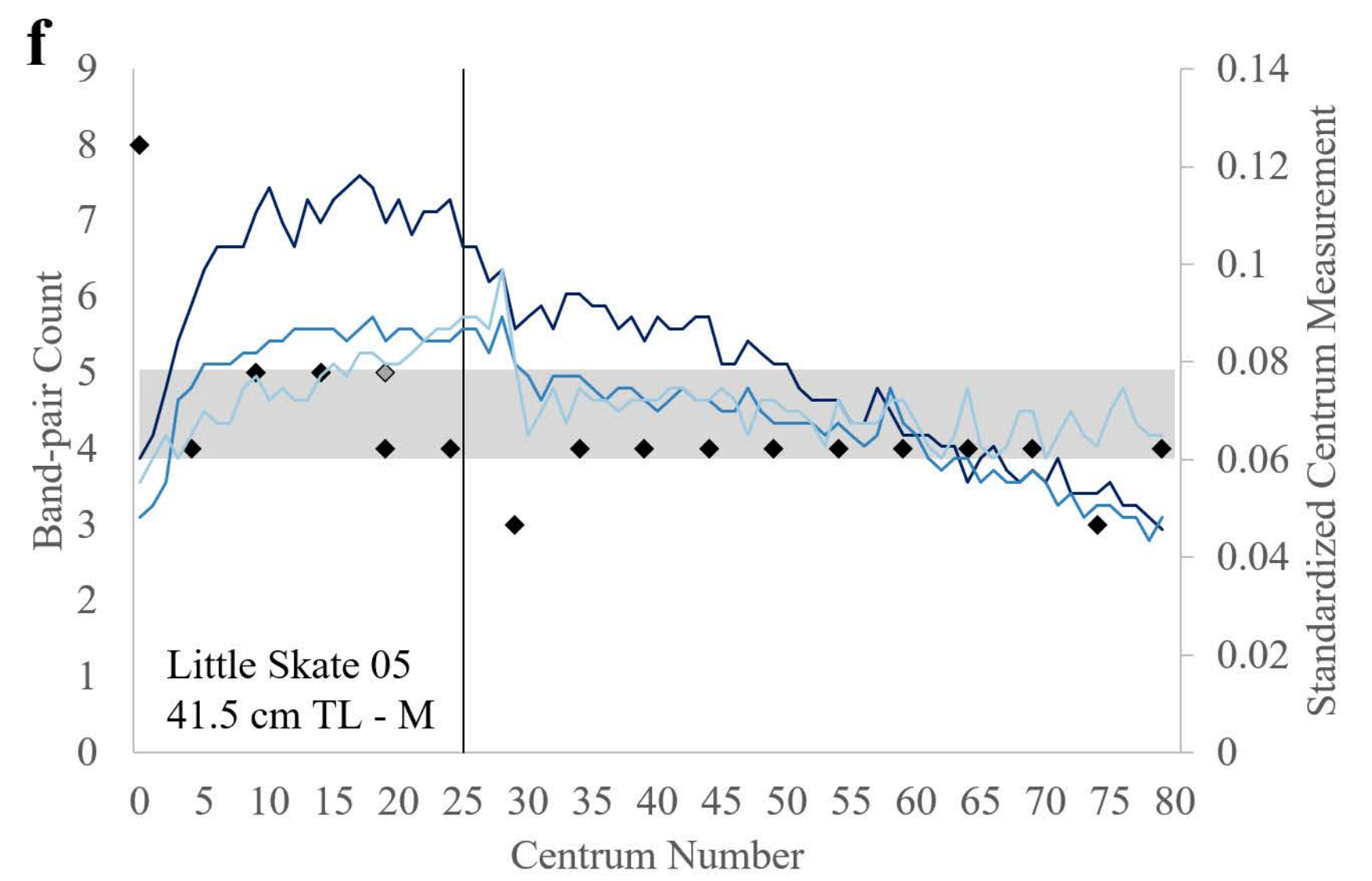
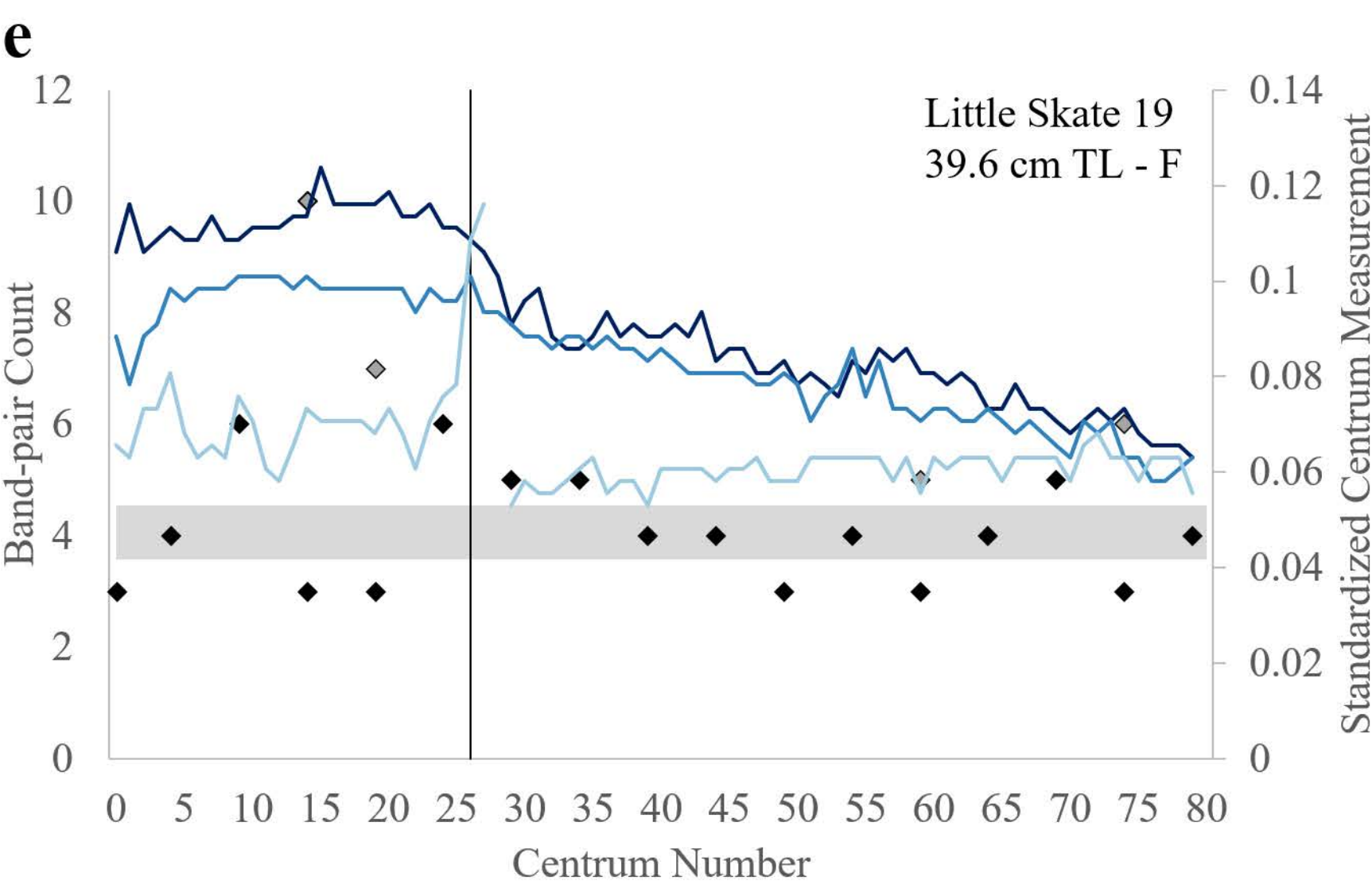
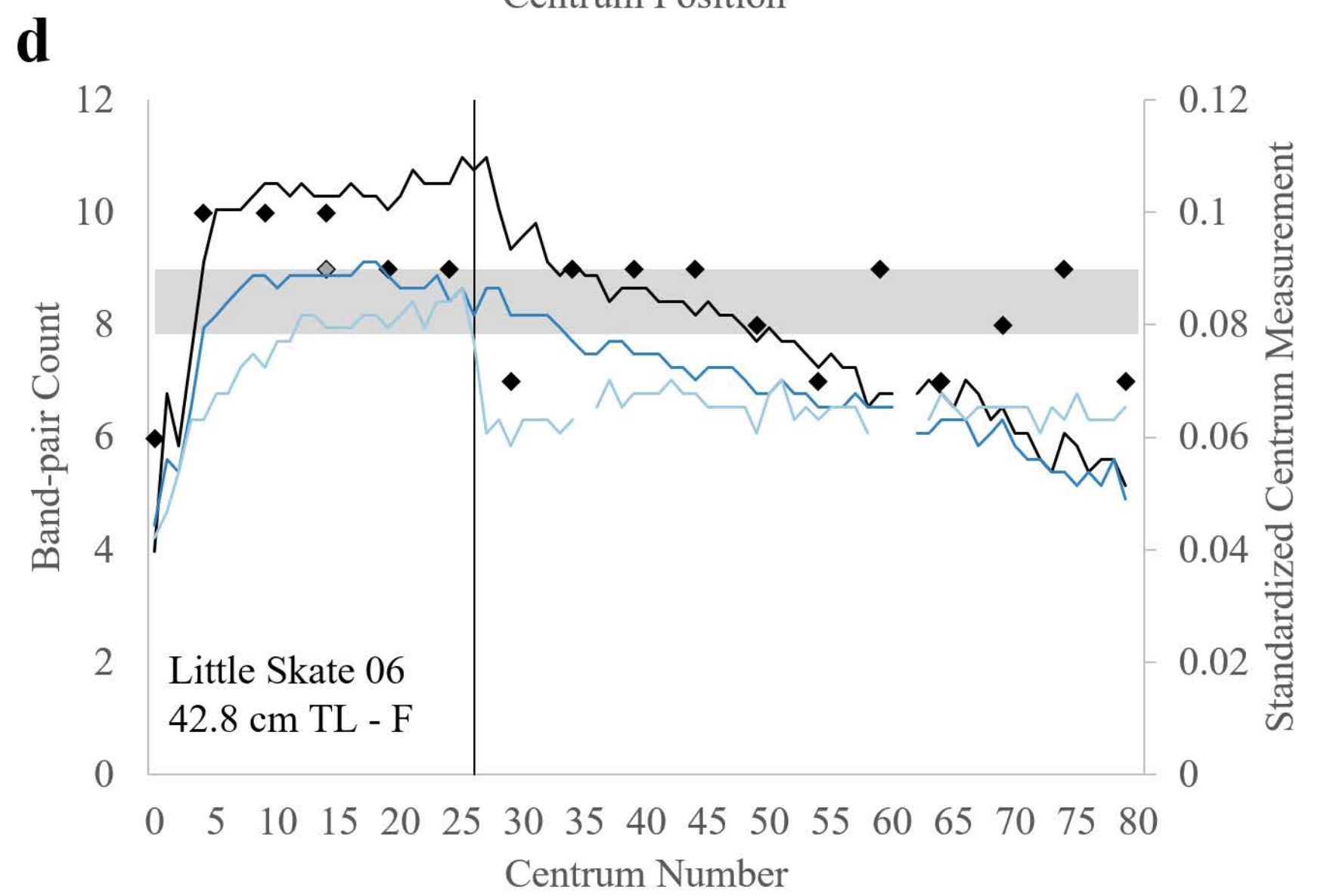
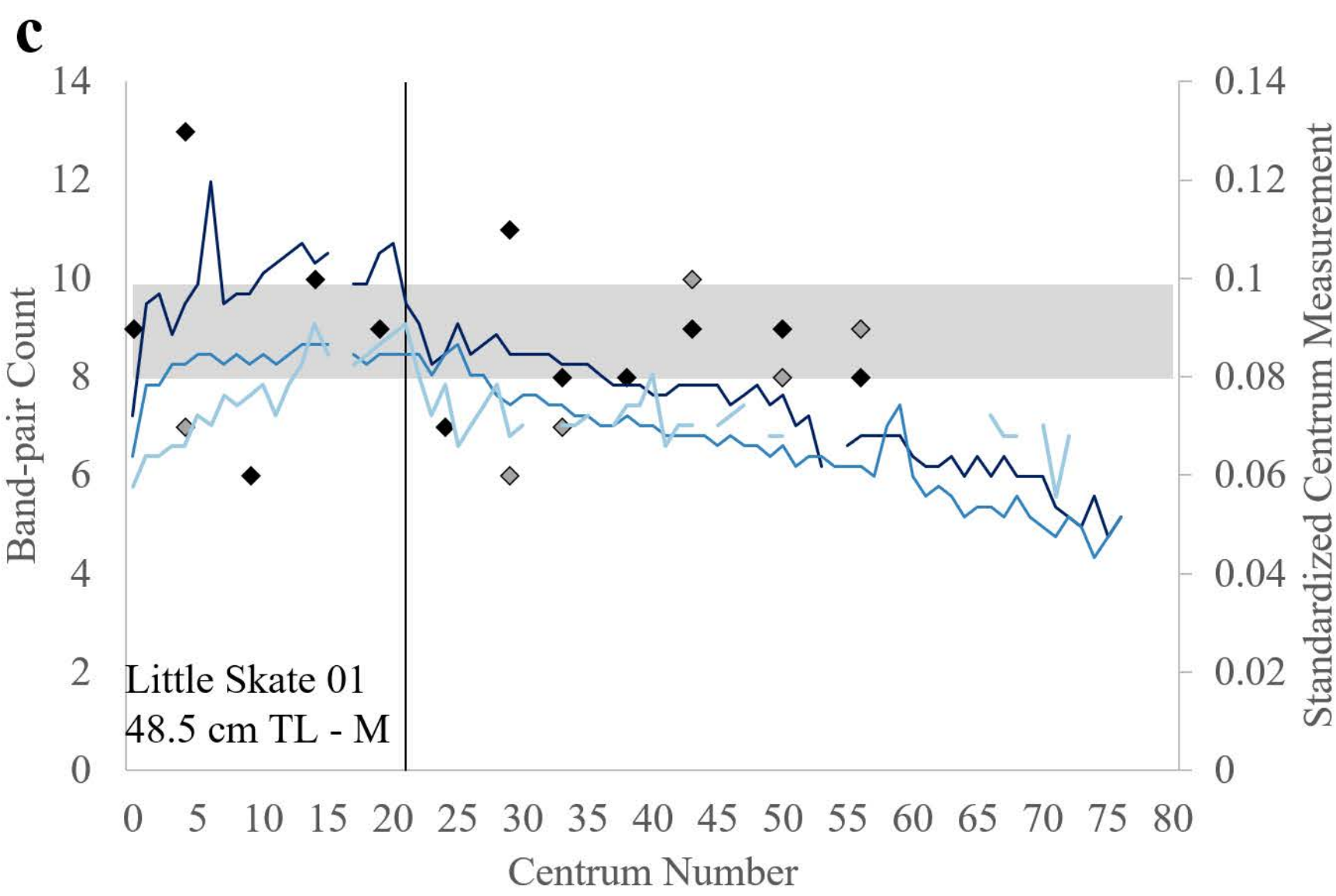
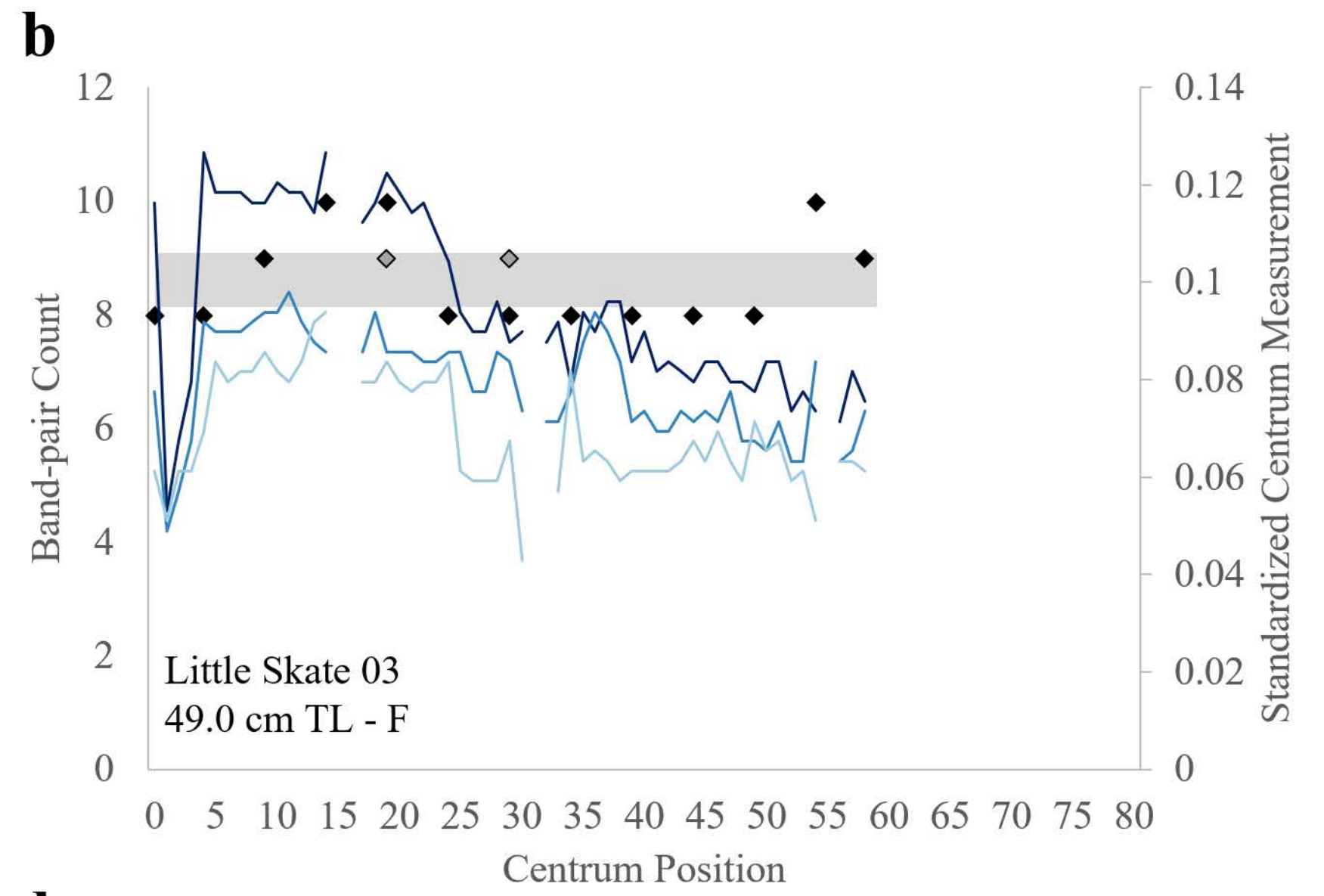
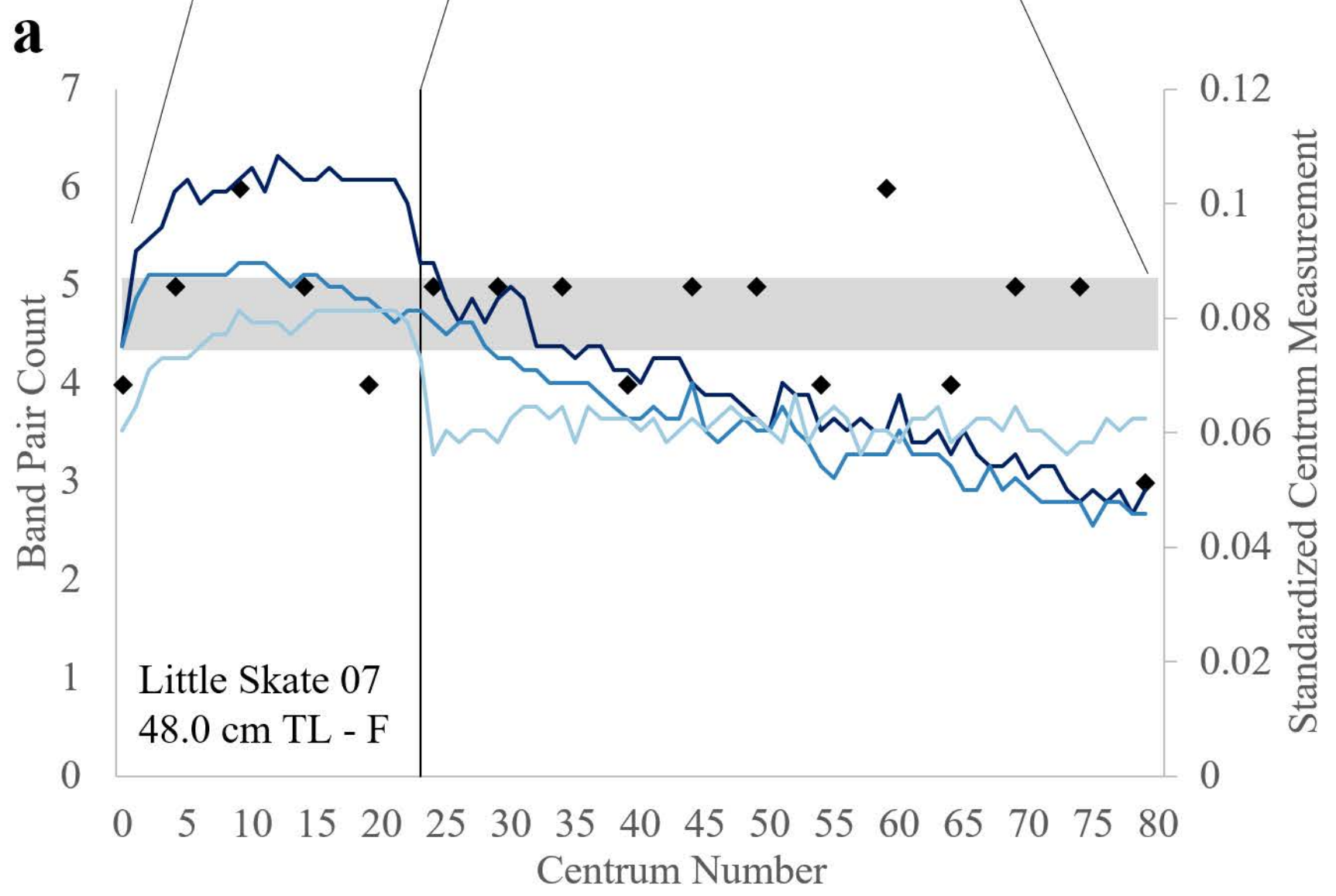




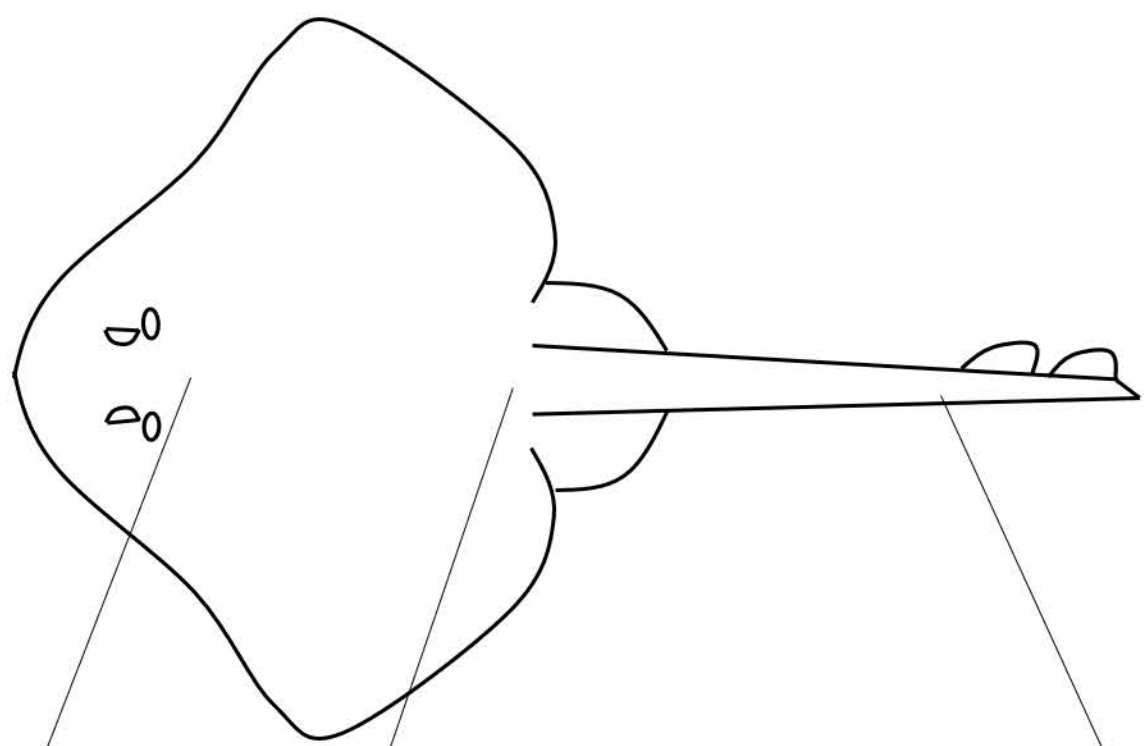


## Legend

- 95% Confidence Interval
- ◆ Primary Band-pair Count
- ◆ Consensus Band-pair Count
- End of Gut Cavity
- Standardized Lateral Diameter
- Standardized Dorsal Diameter
- Standardized Length

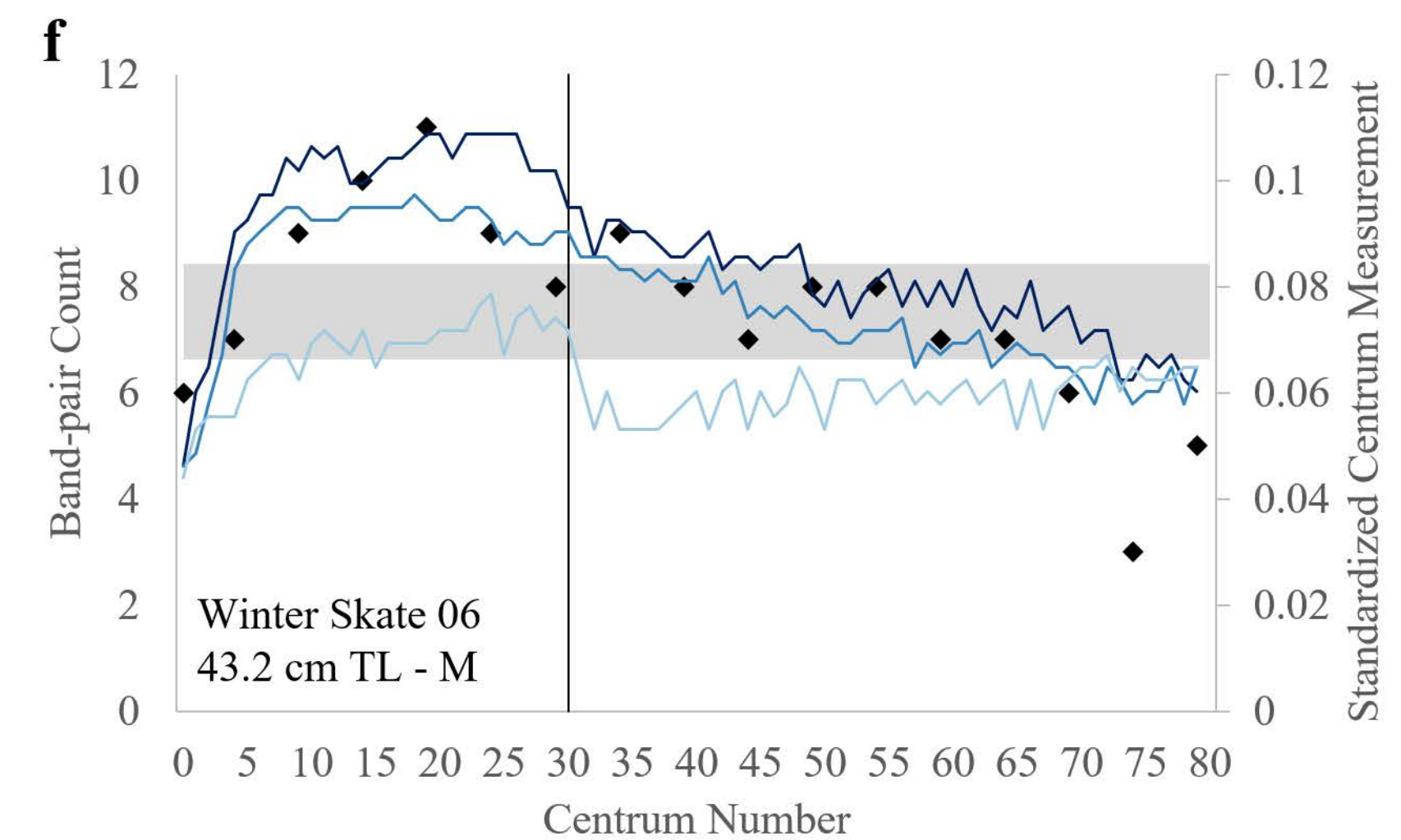
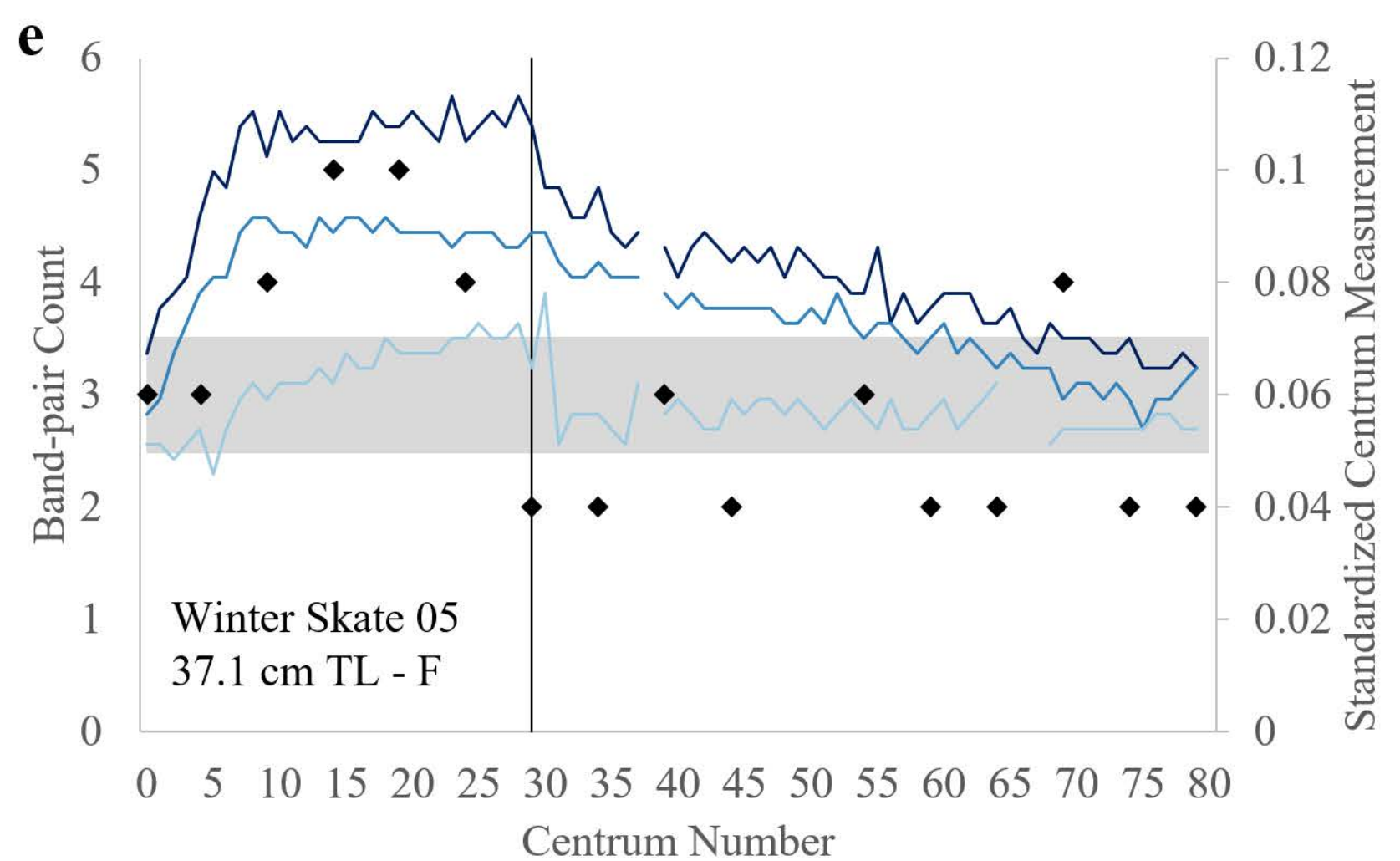
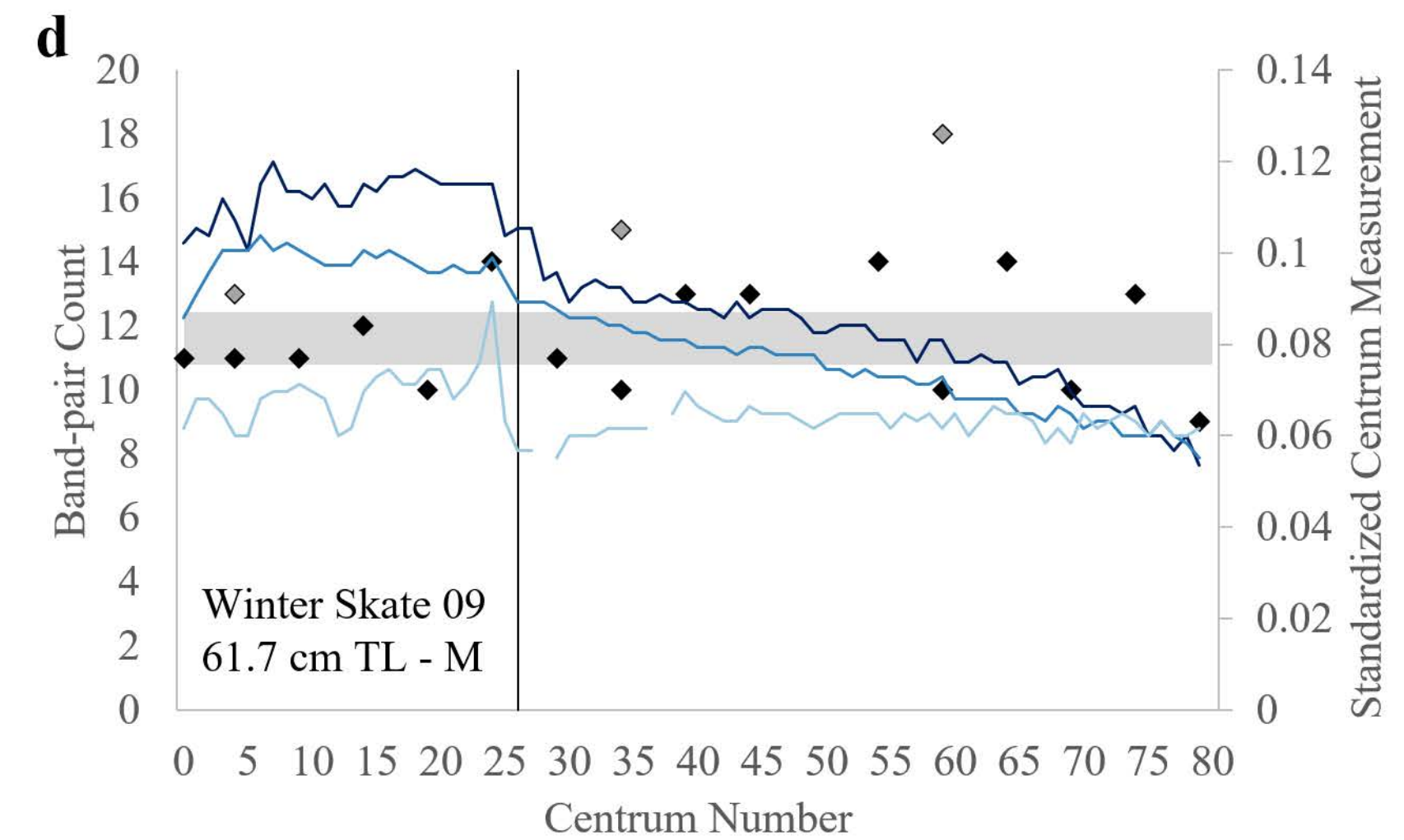
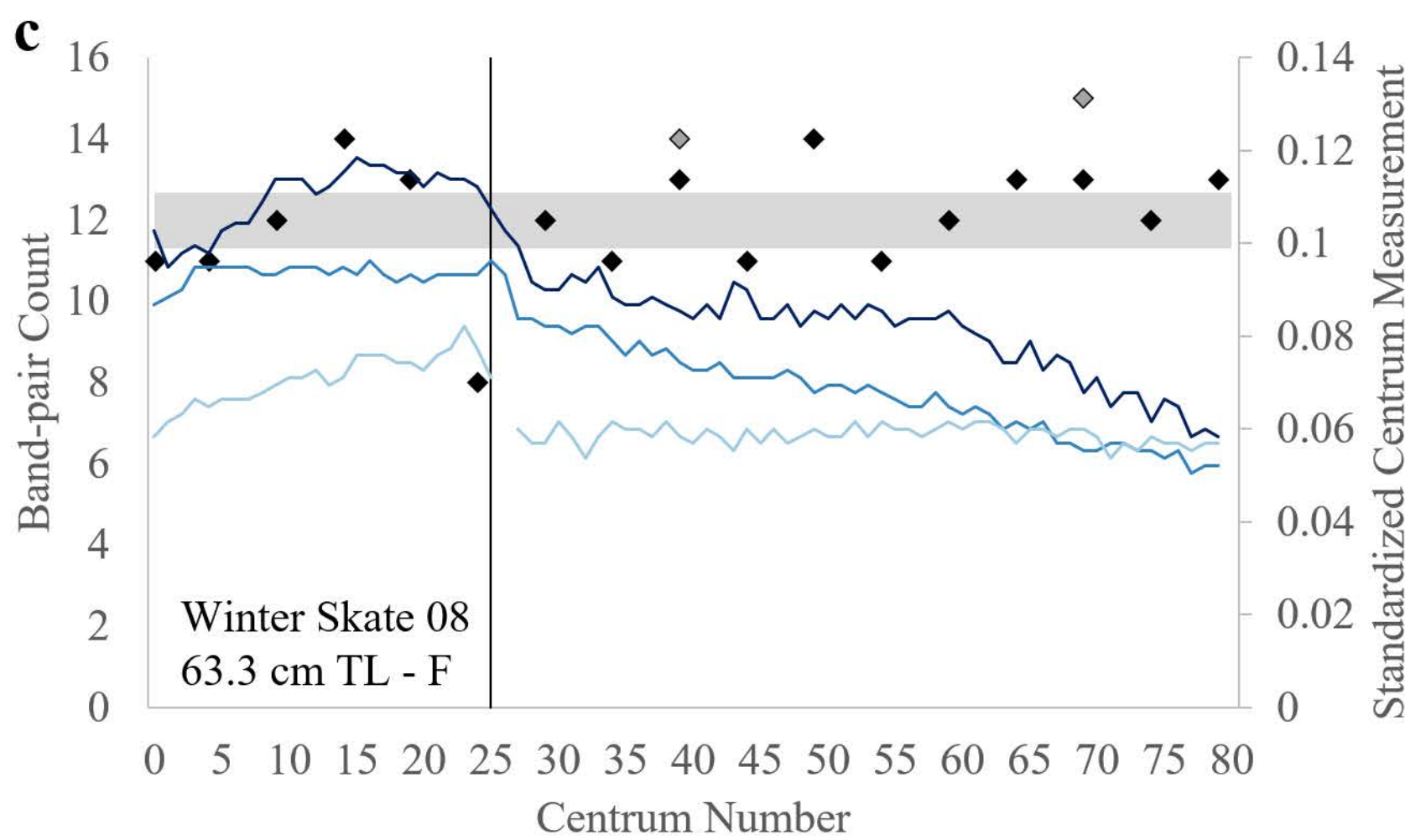
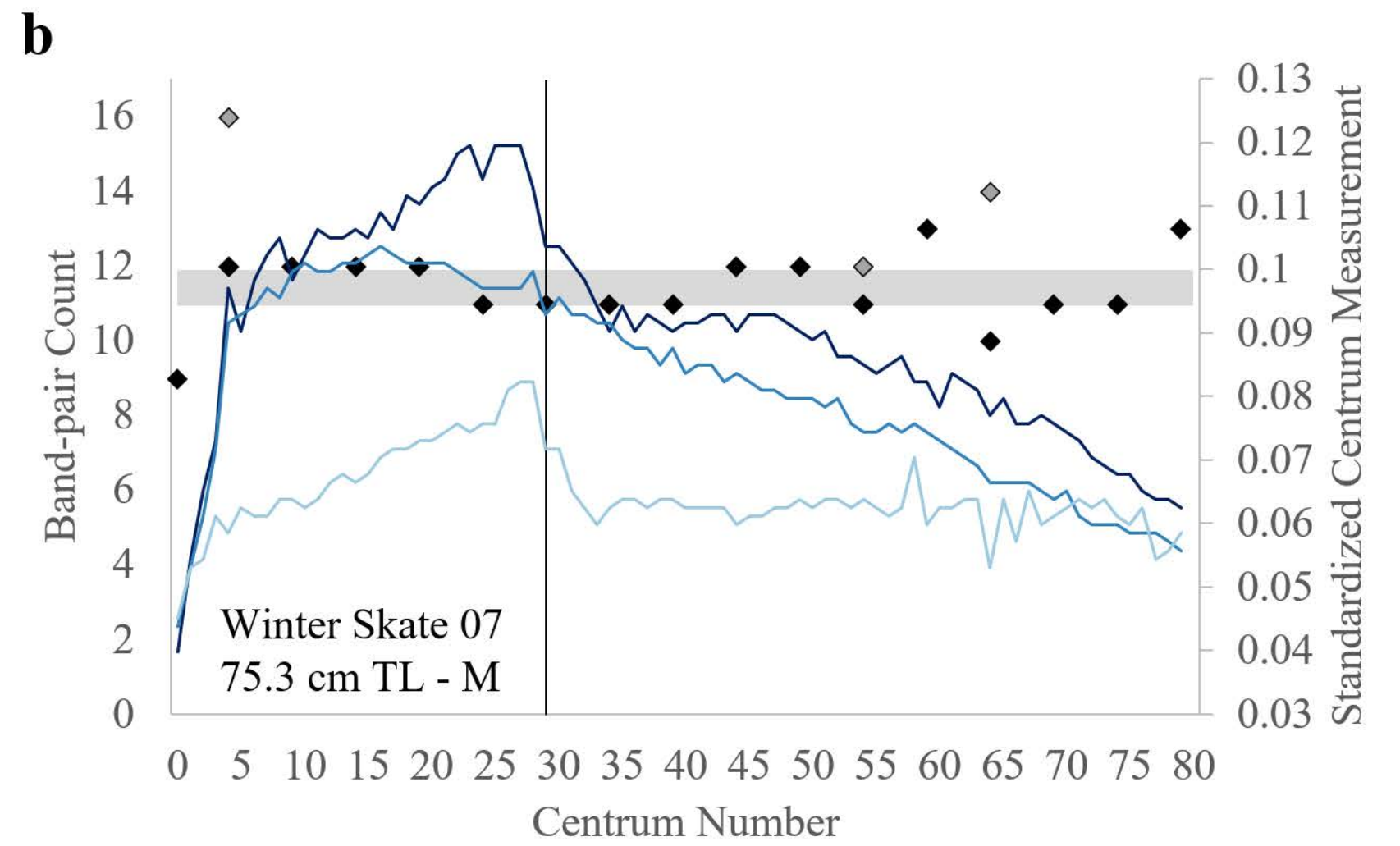
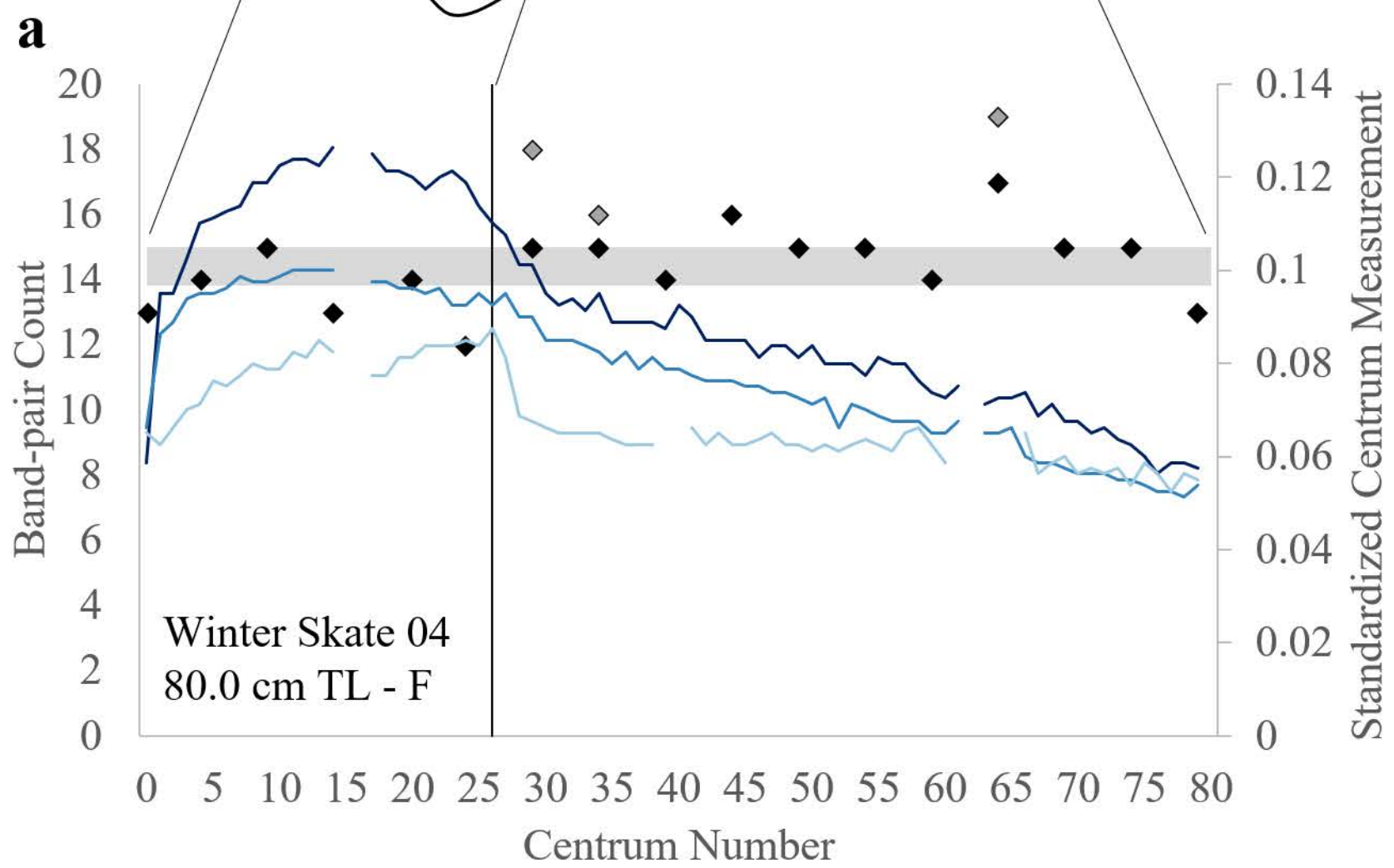




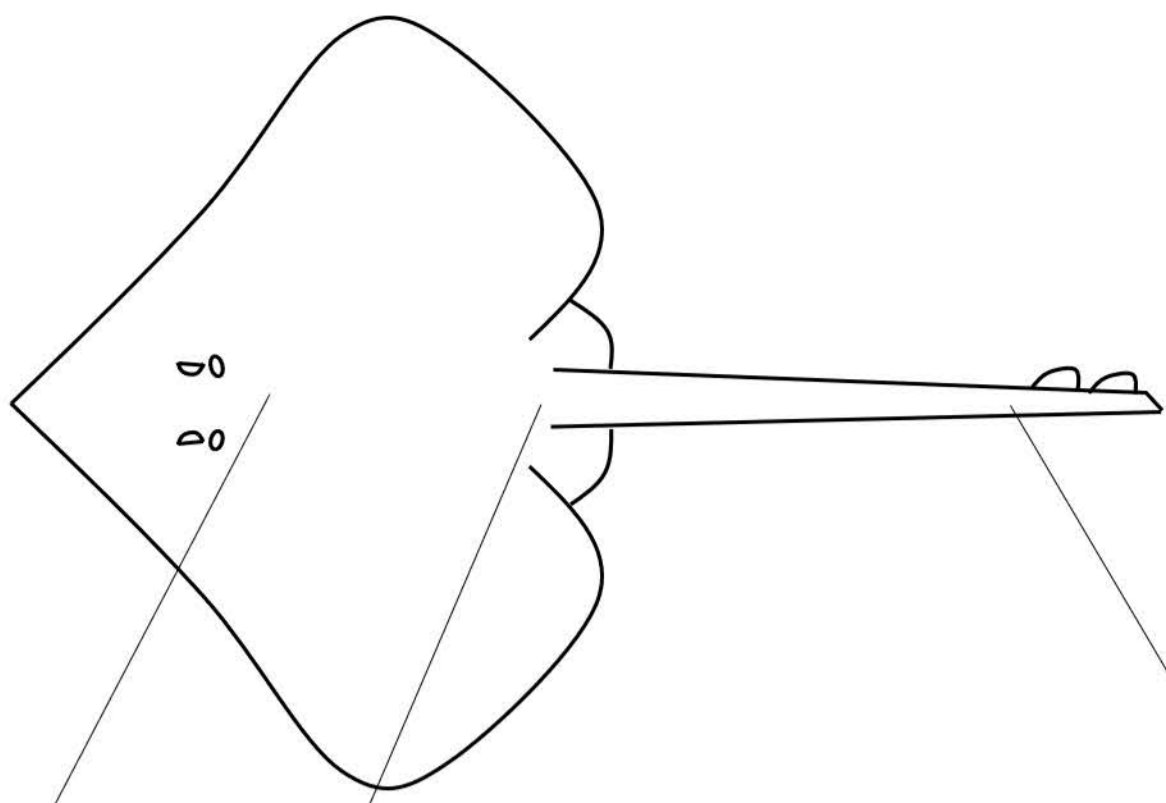


## Legend

- 95% Confidence Interval
- ◆ Consensus Band-pair Count
- End of Gut Cavity
- Standardized Lateral Diameter
- Standardized Dorsal Diameter
- Standardized Length
- ◆ Primary Band-pair Count

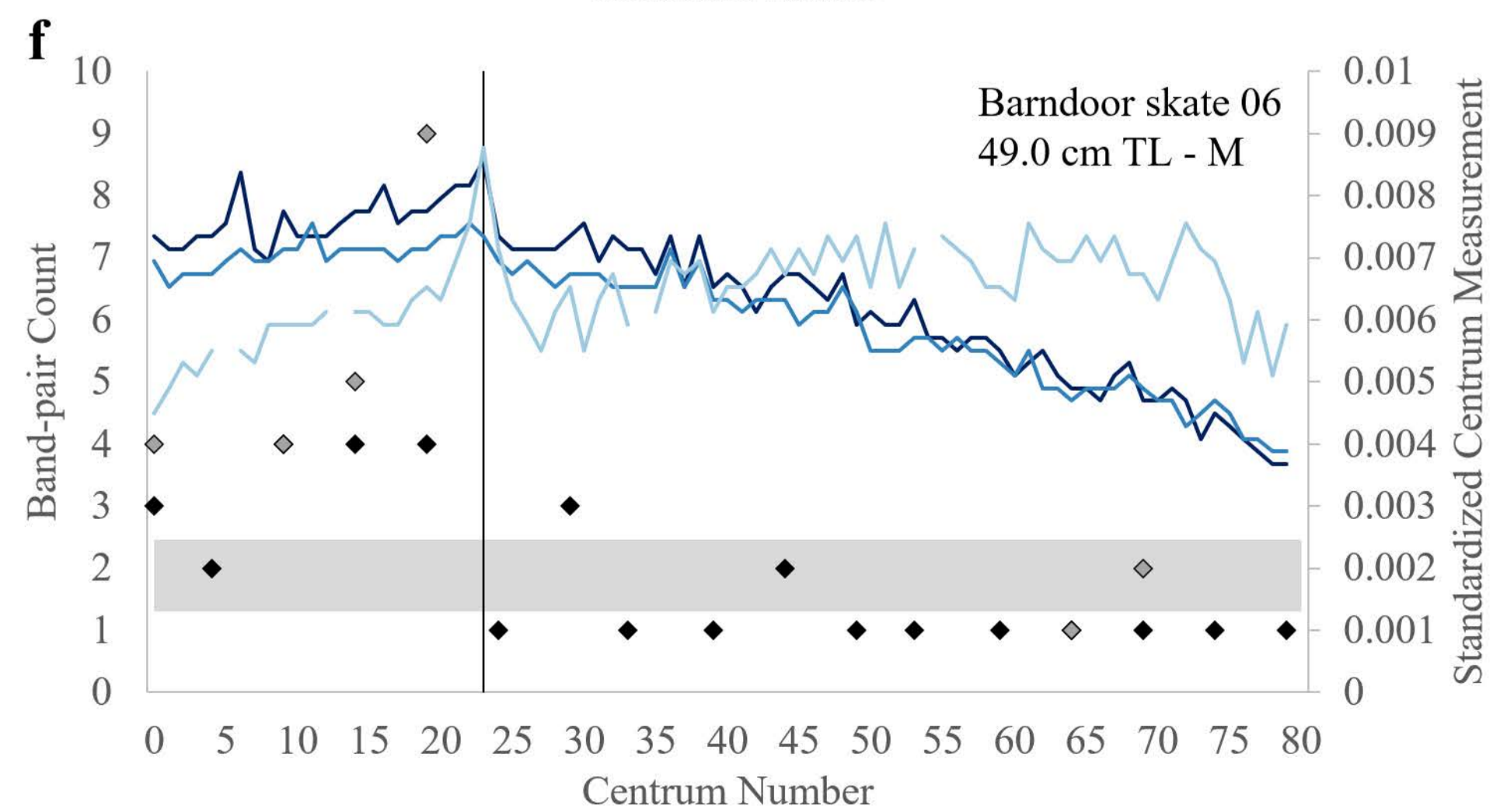
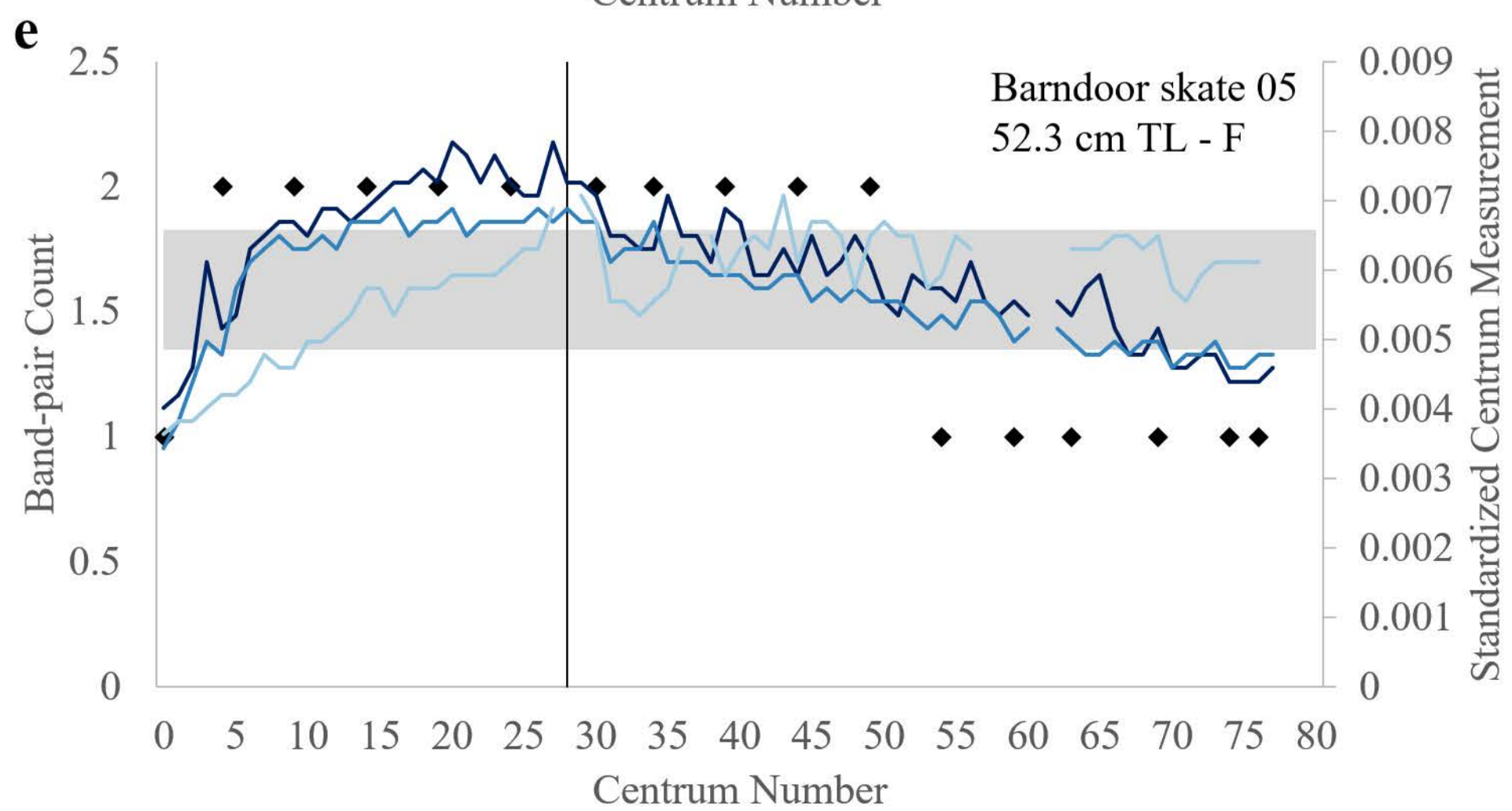
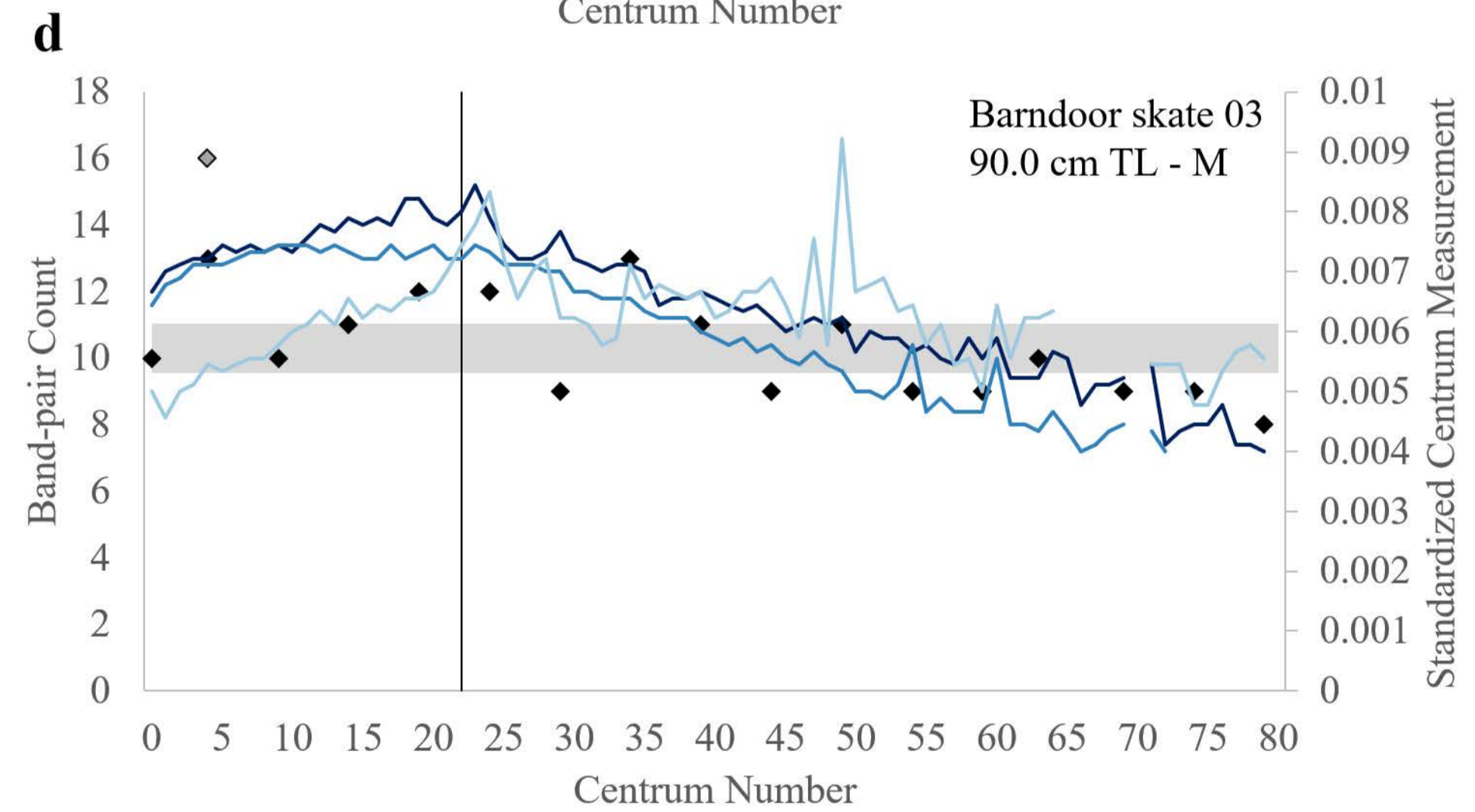
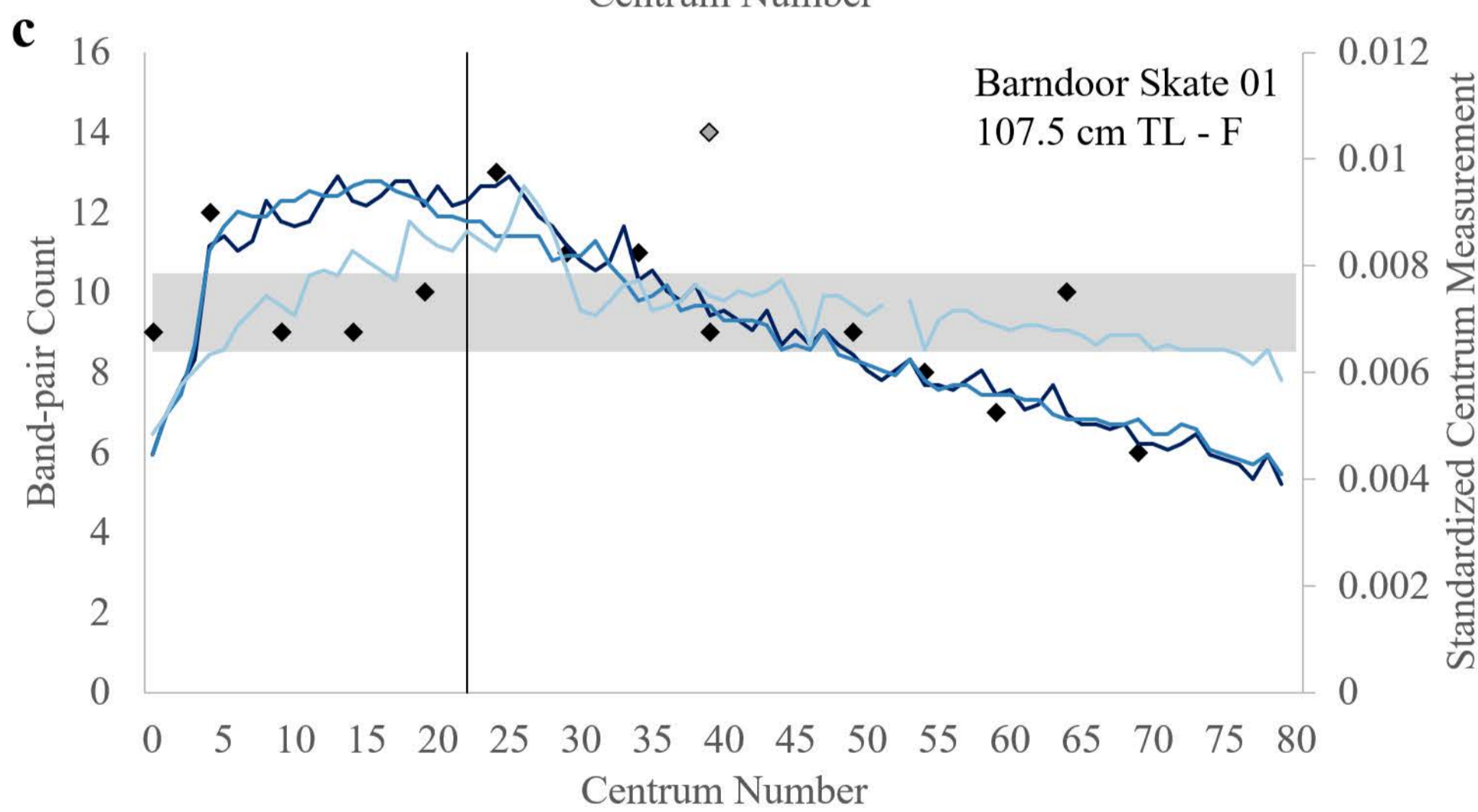
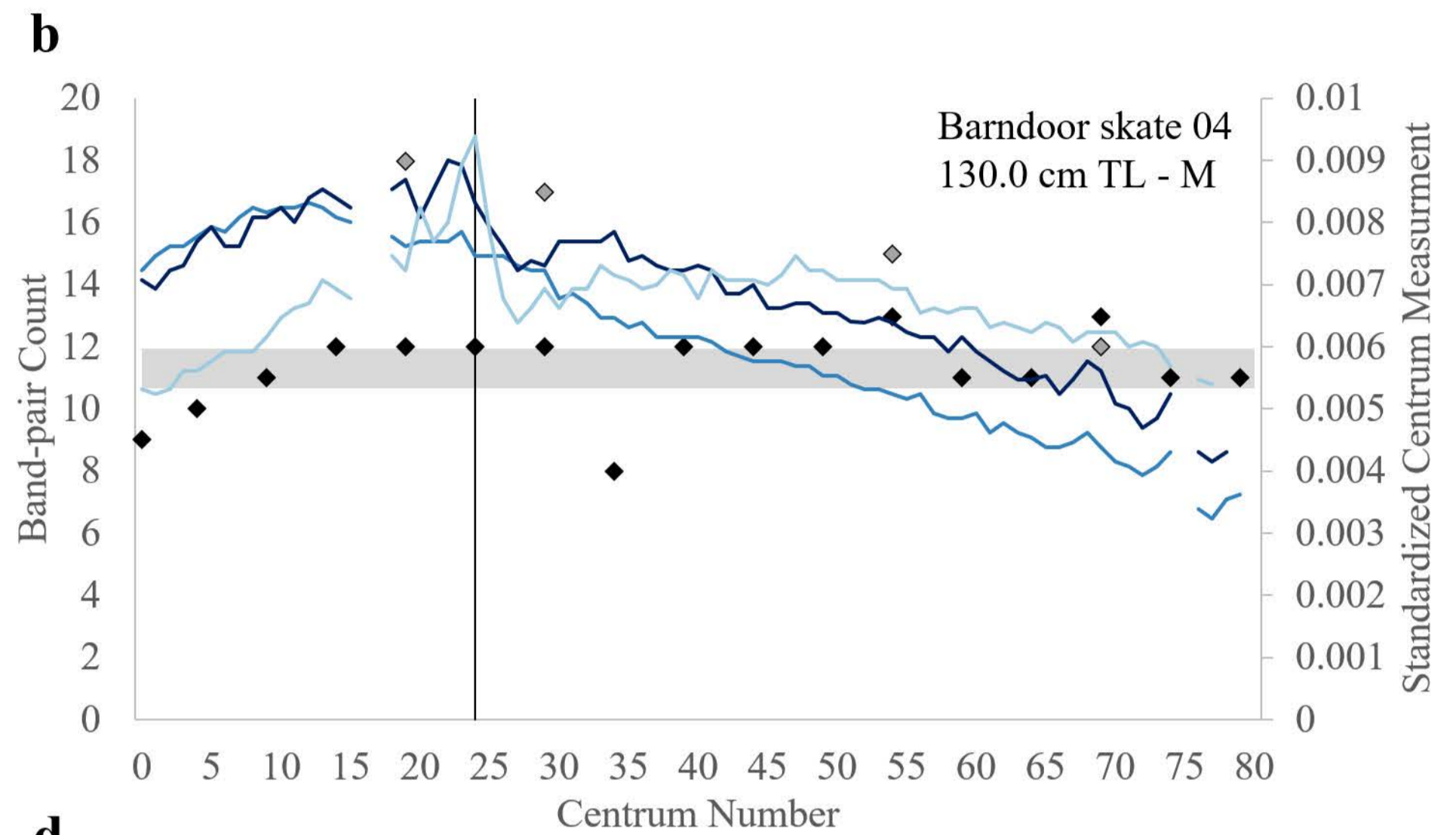
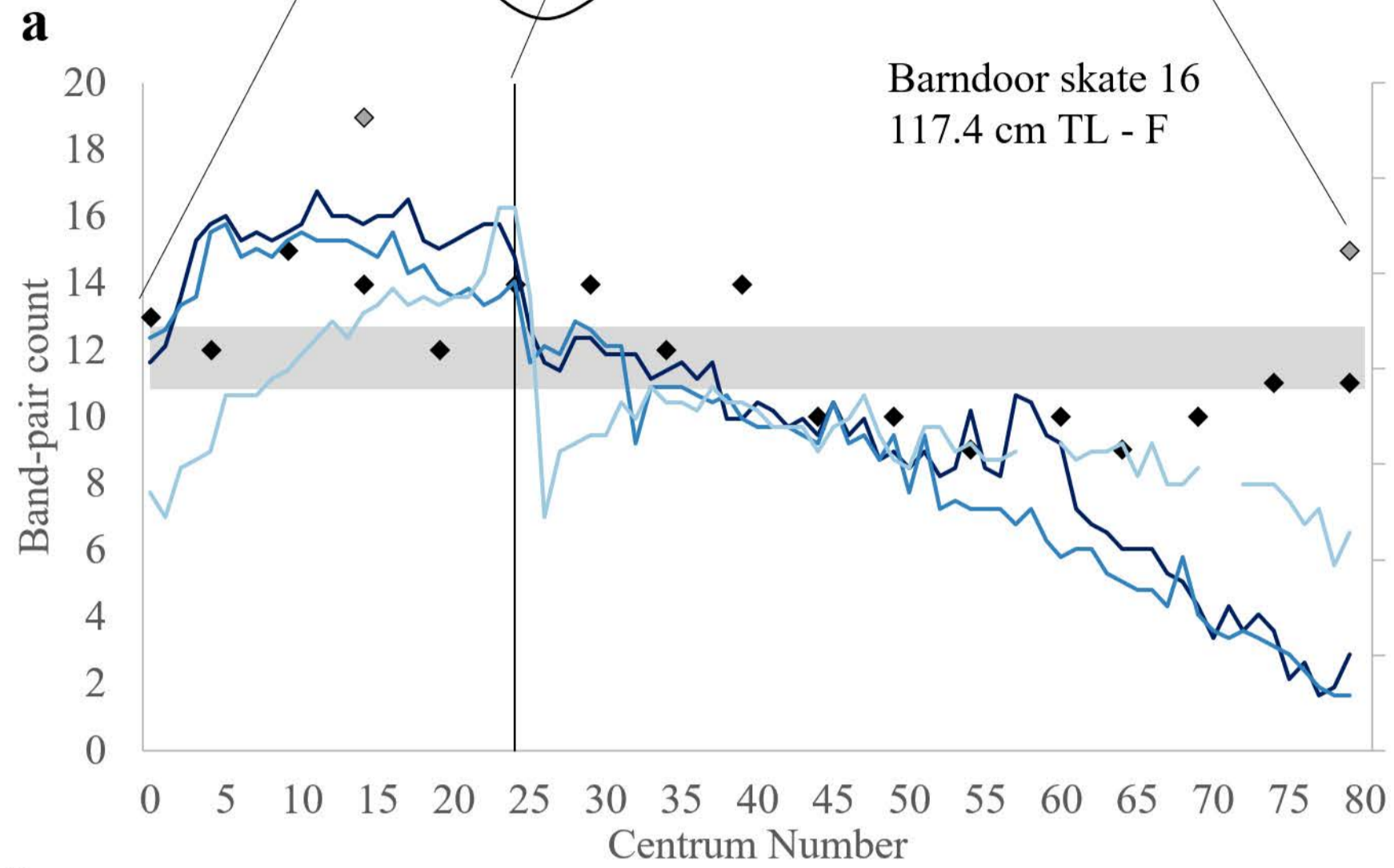






## Legend

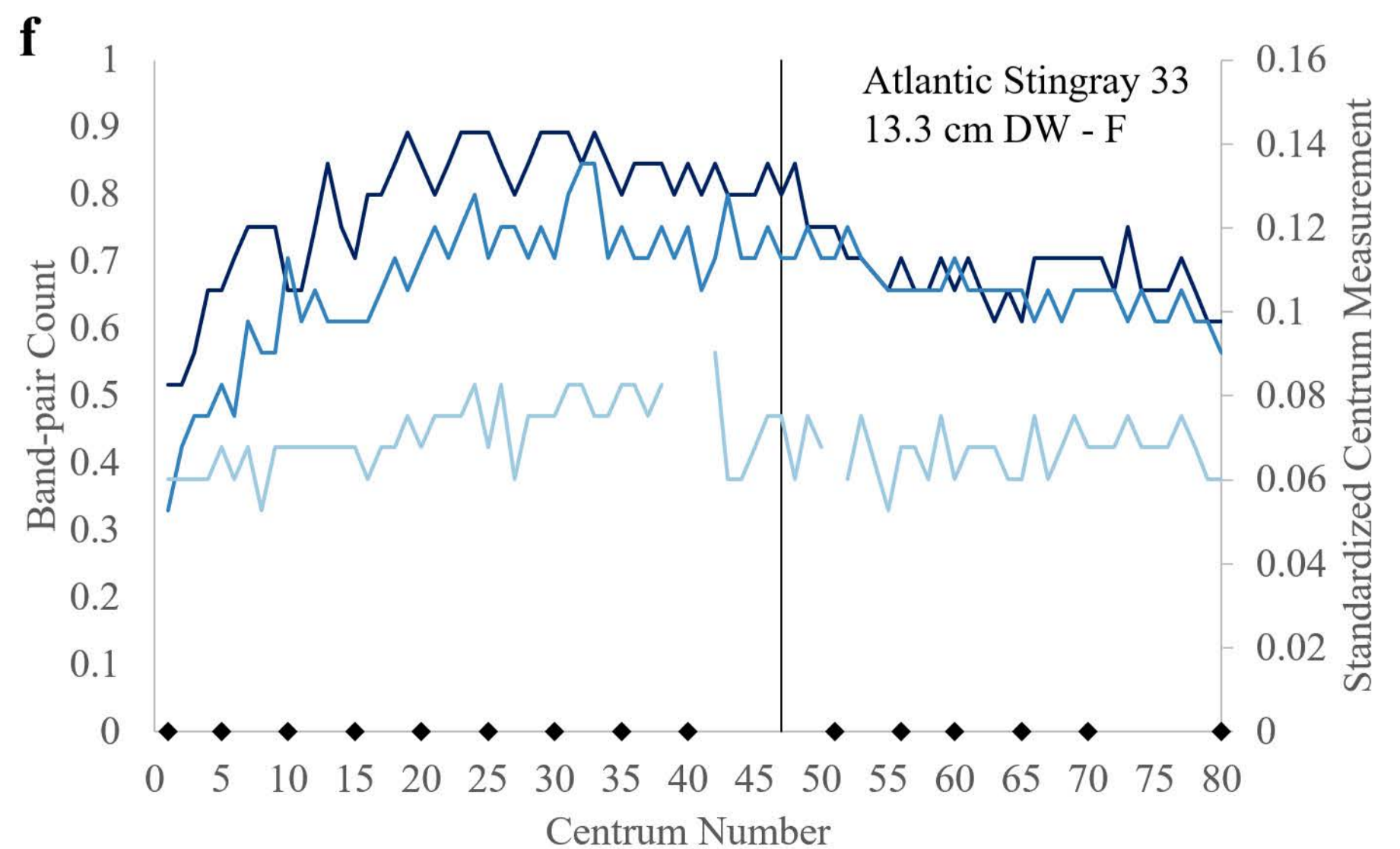
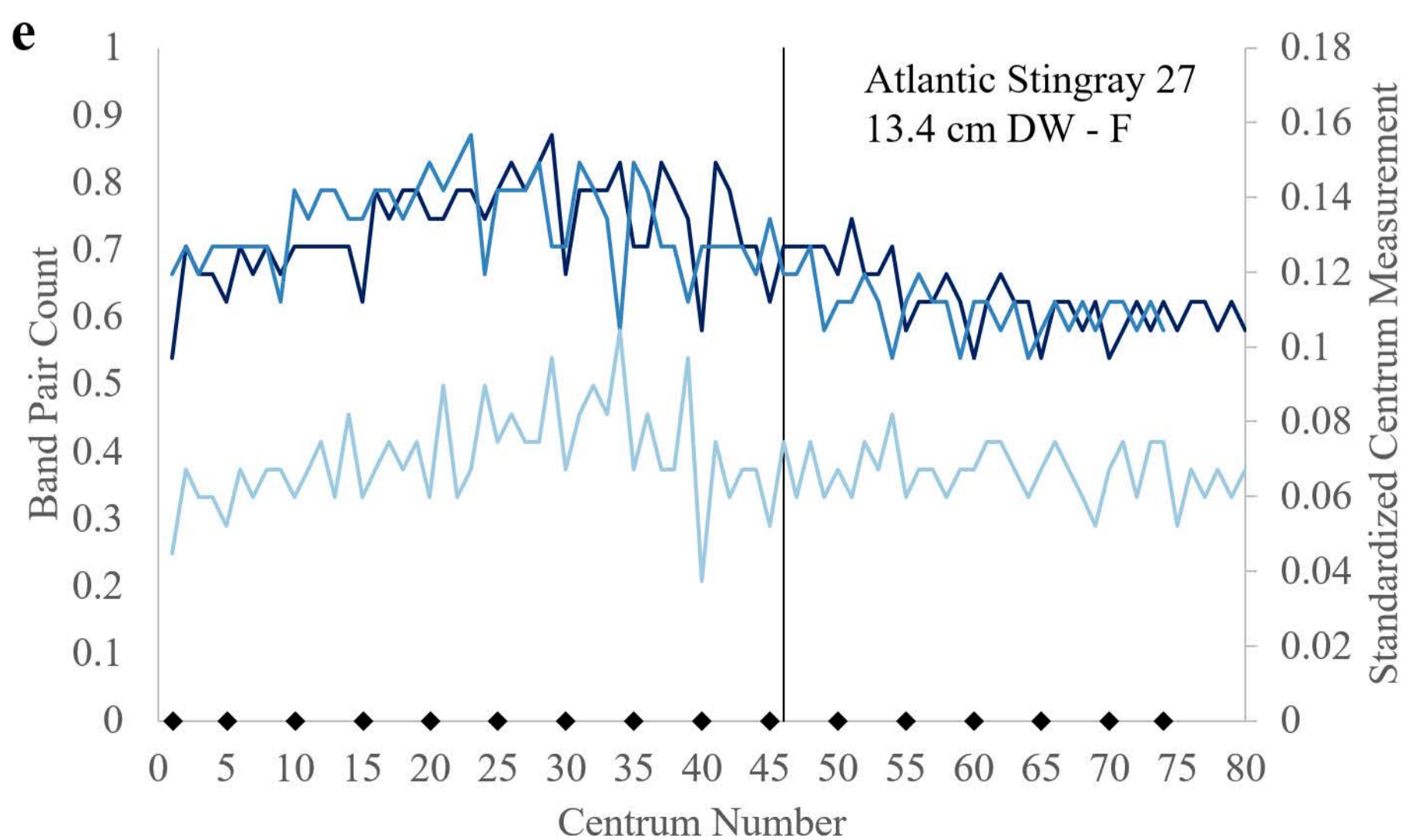
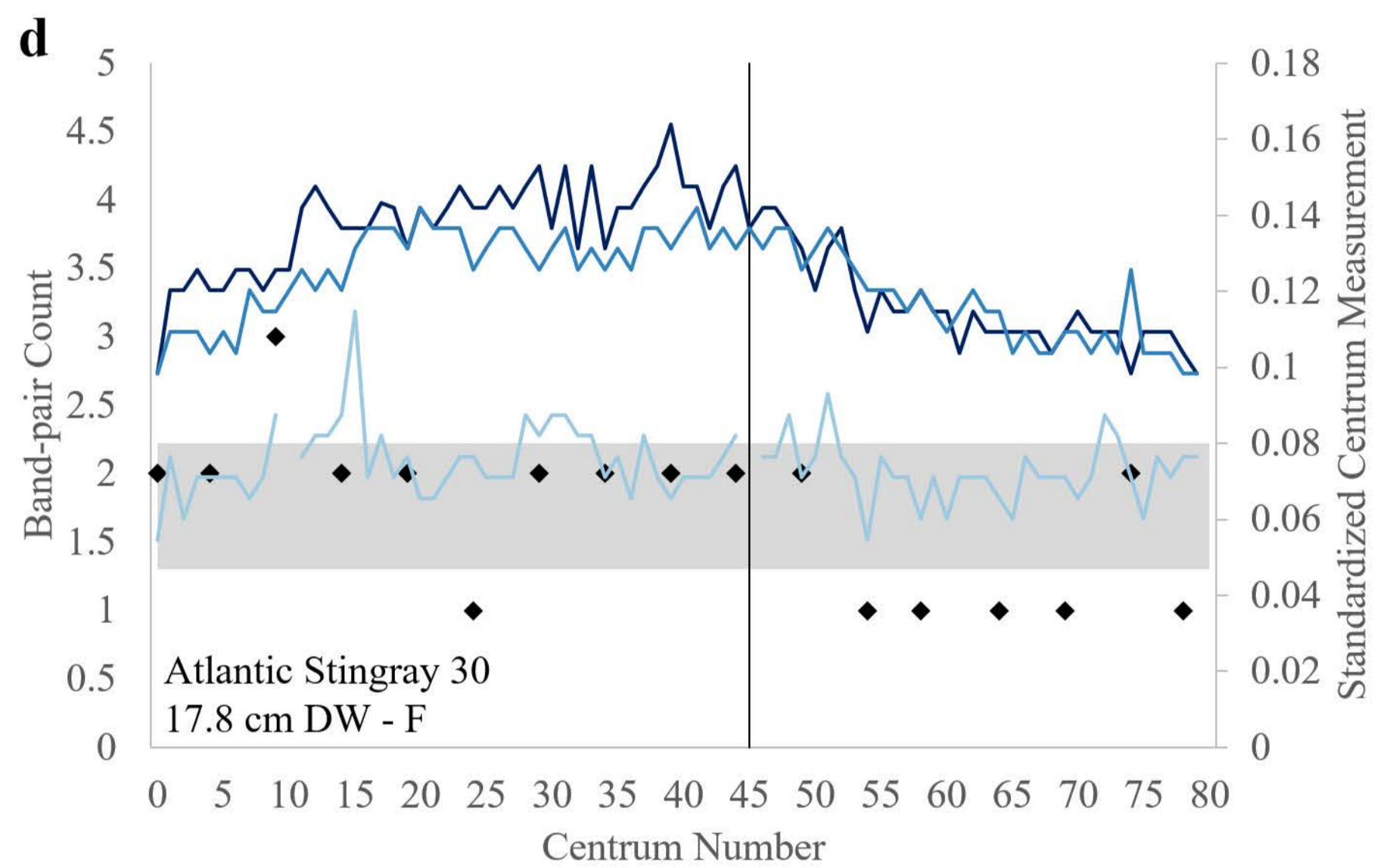
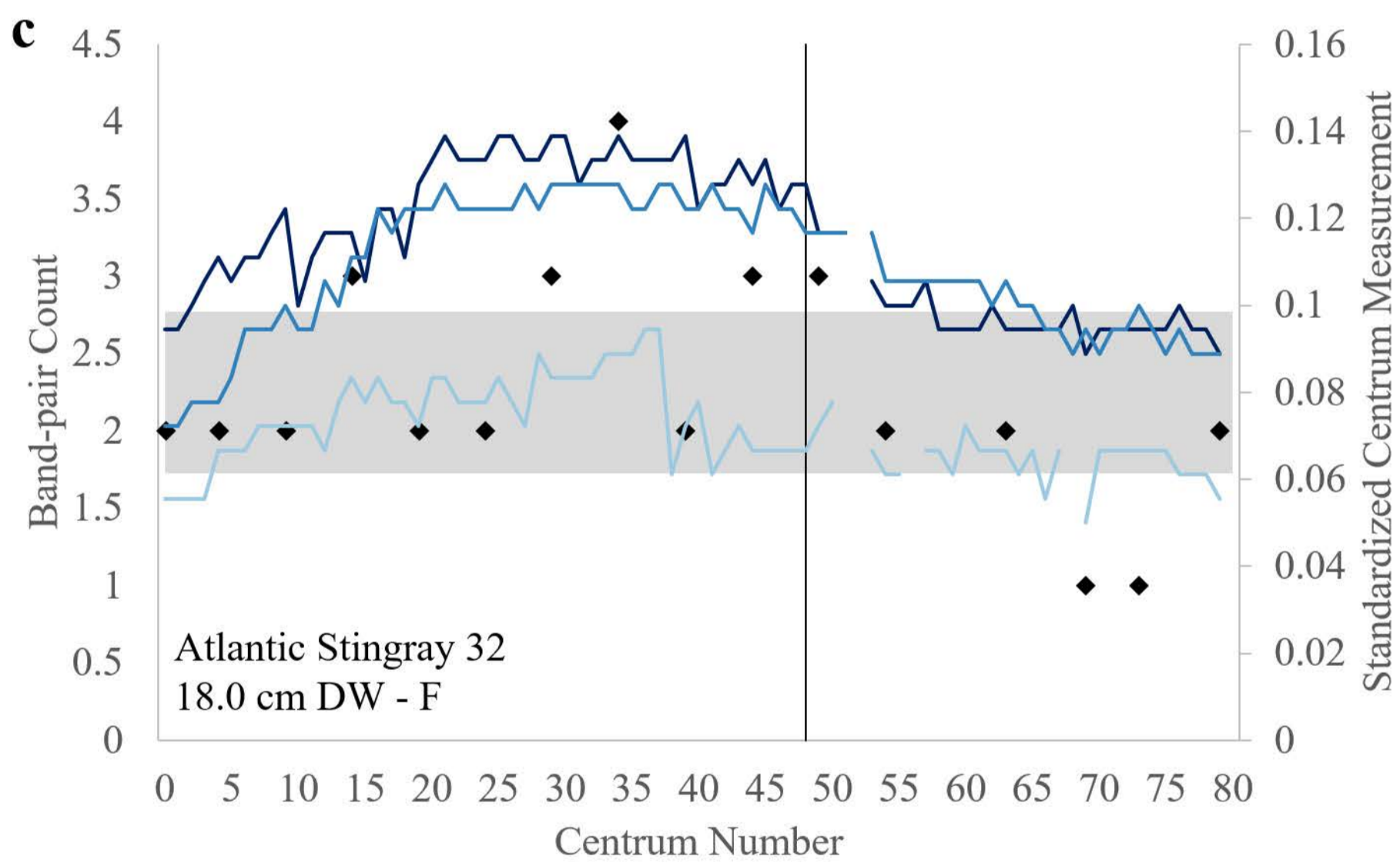
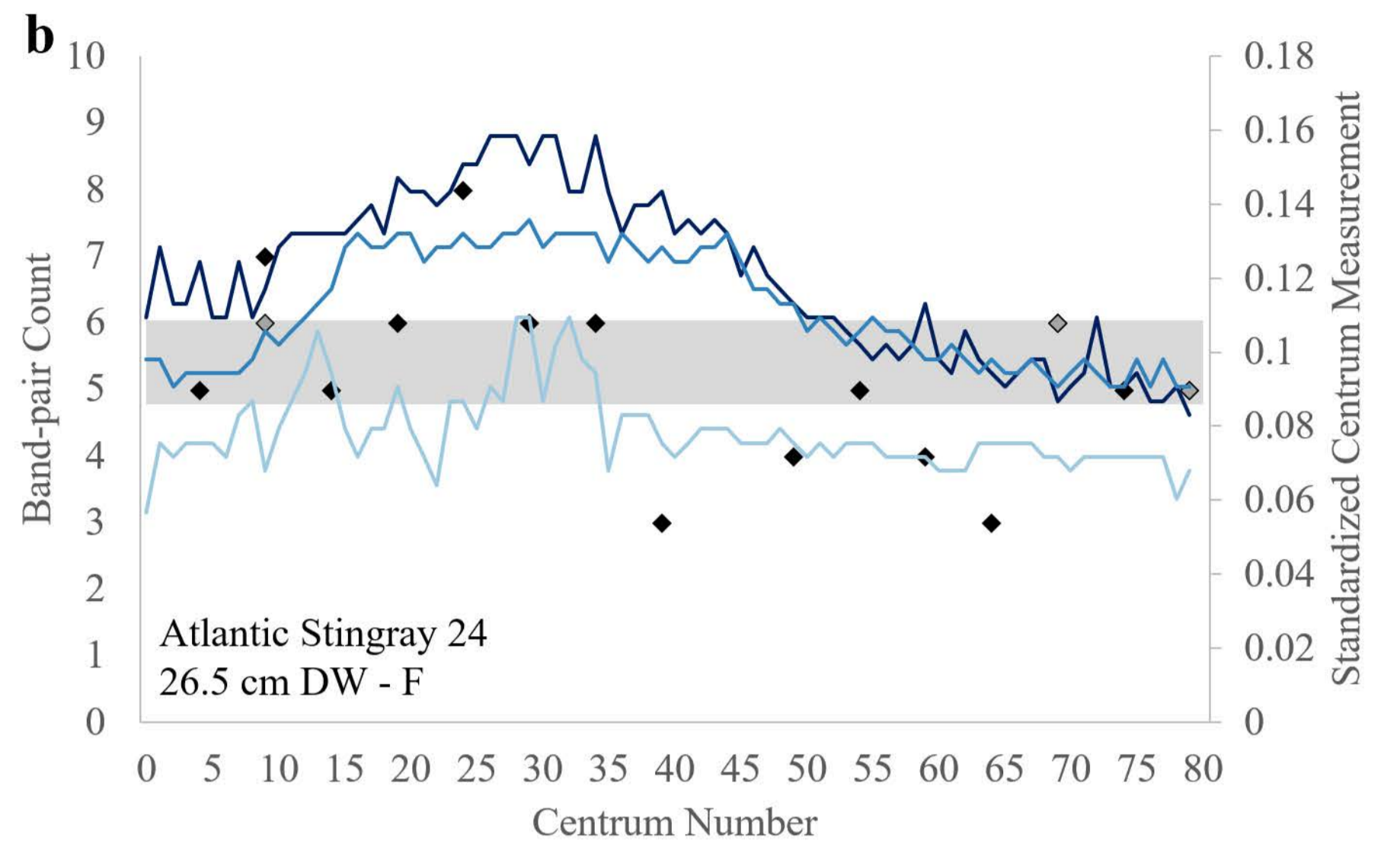
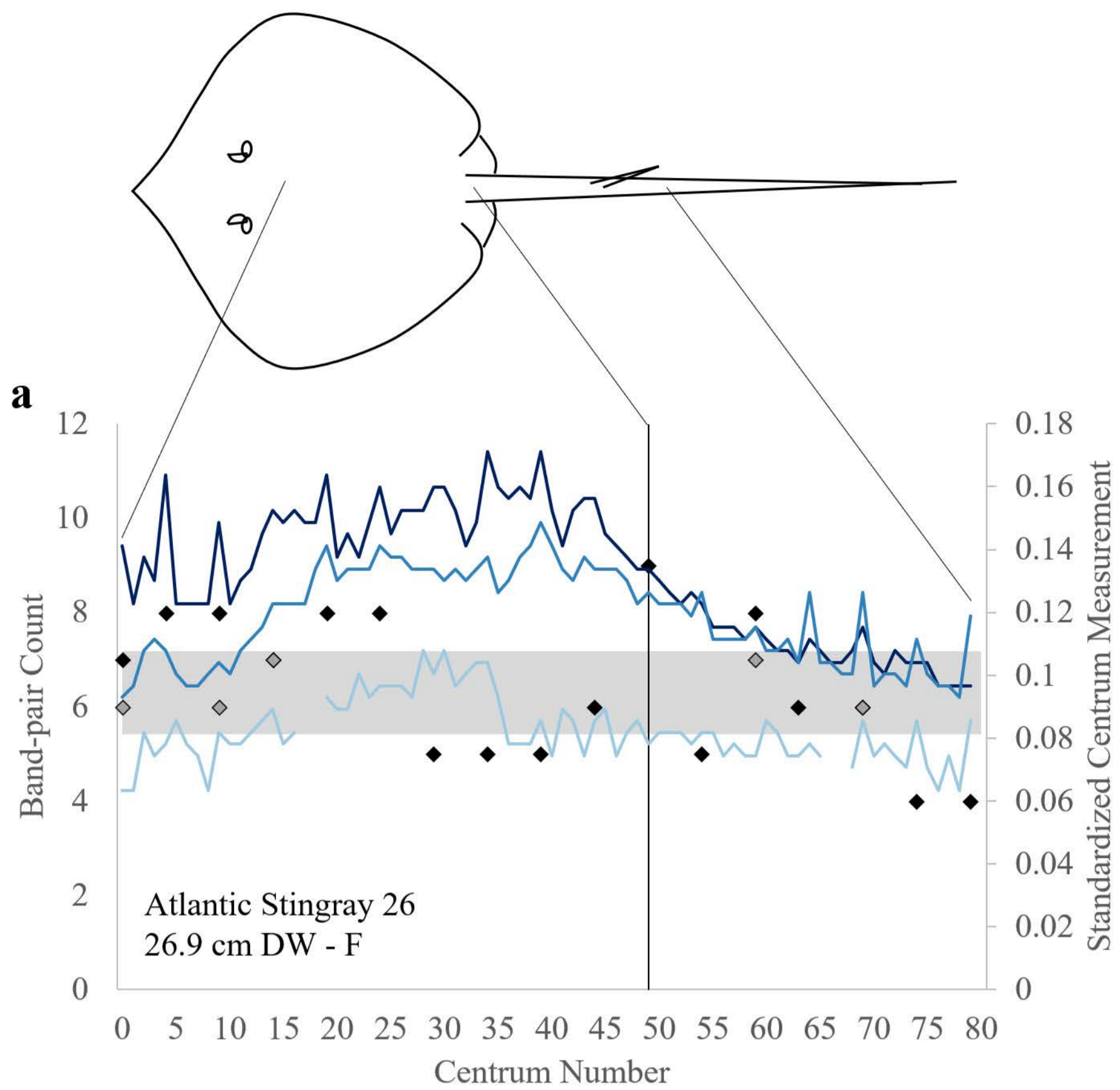
- 95% Confidence Interval
- ◆ Primary Band-pair Count
- ◆ Consensus Band-pair Count
- End of gut cavity
- Standardized Lateral Diameter
- Standardized Dorsal Diameter
- Standardized Length



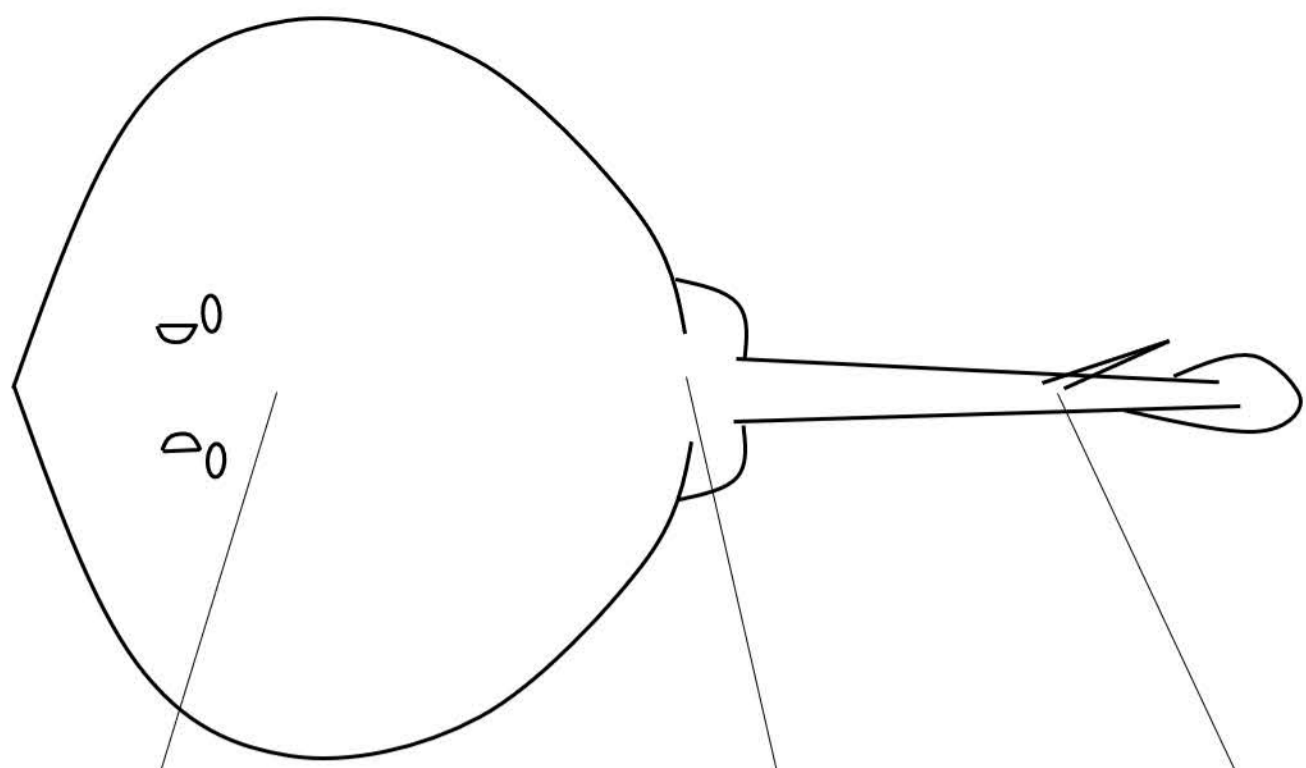


## Legend

- 95% Confidence Interval
- ◆ Primary Band-pair Count
- ◇ Consensus Band-pair Count
- End of Gut Cavity
- Standardized Lateral Diameter
- Standardized Dorsal Diameter
- Standardized Length

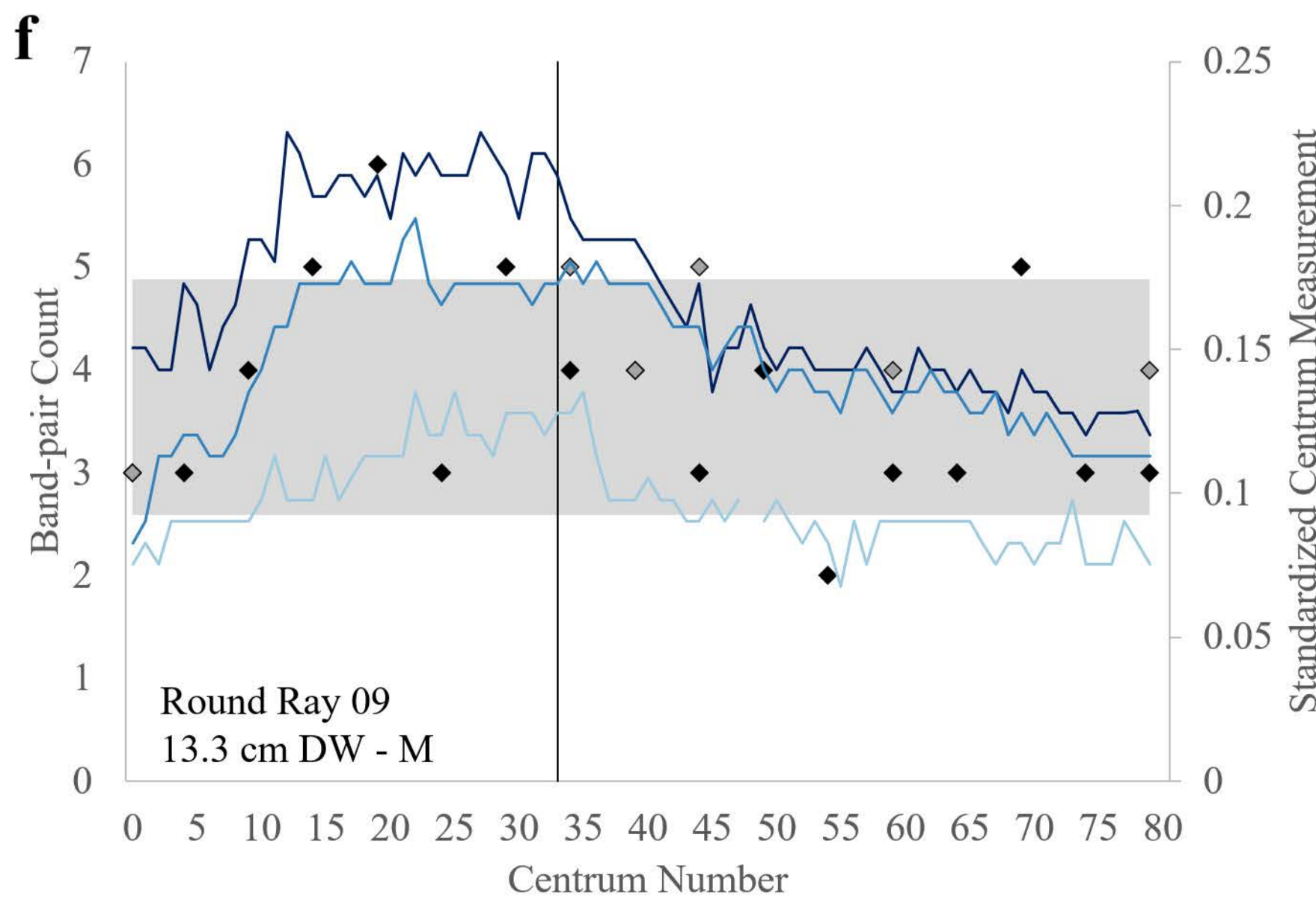
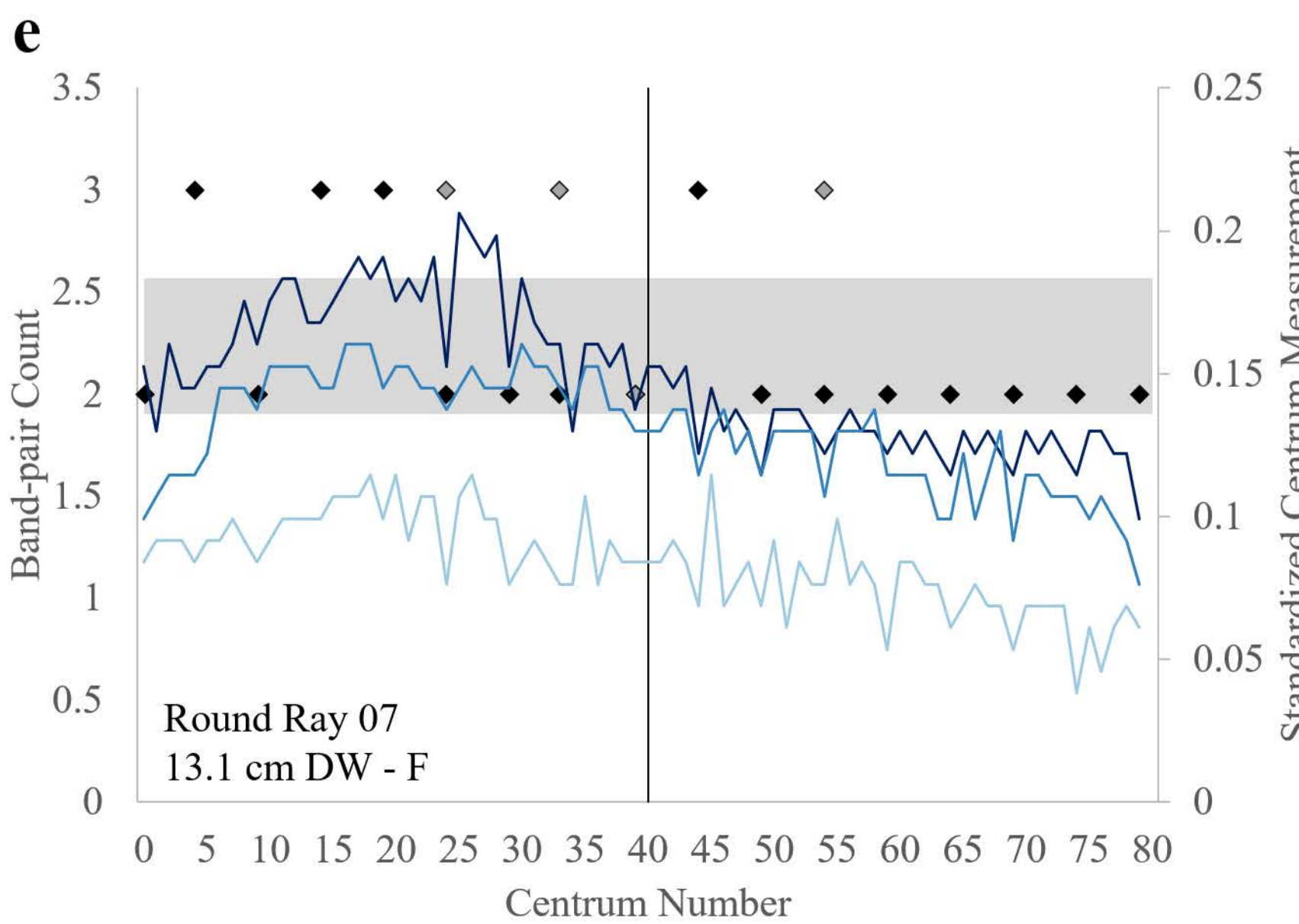
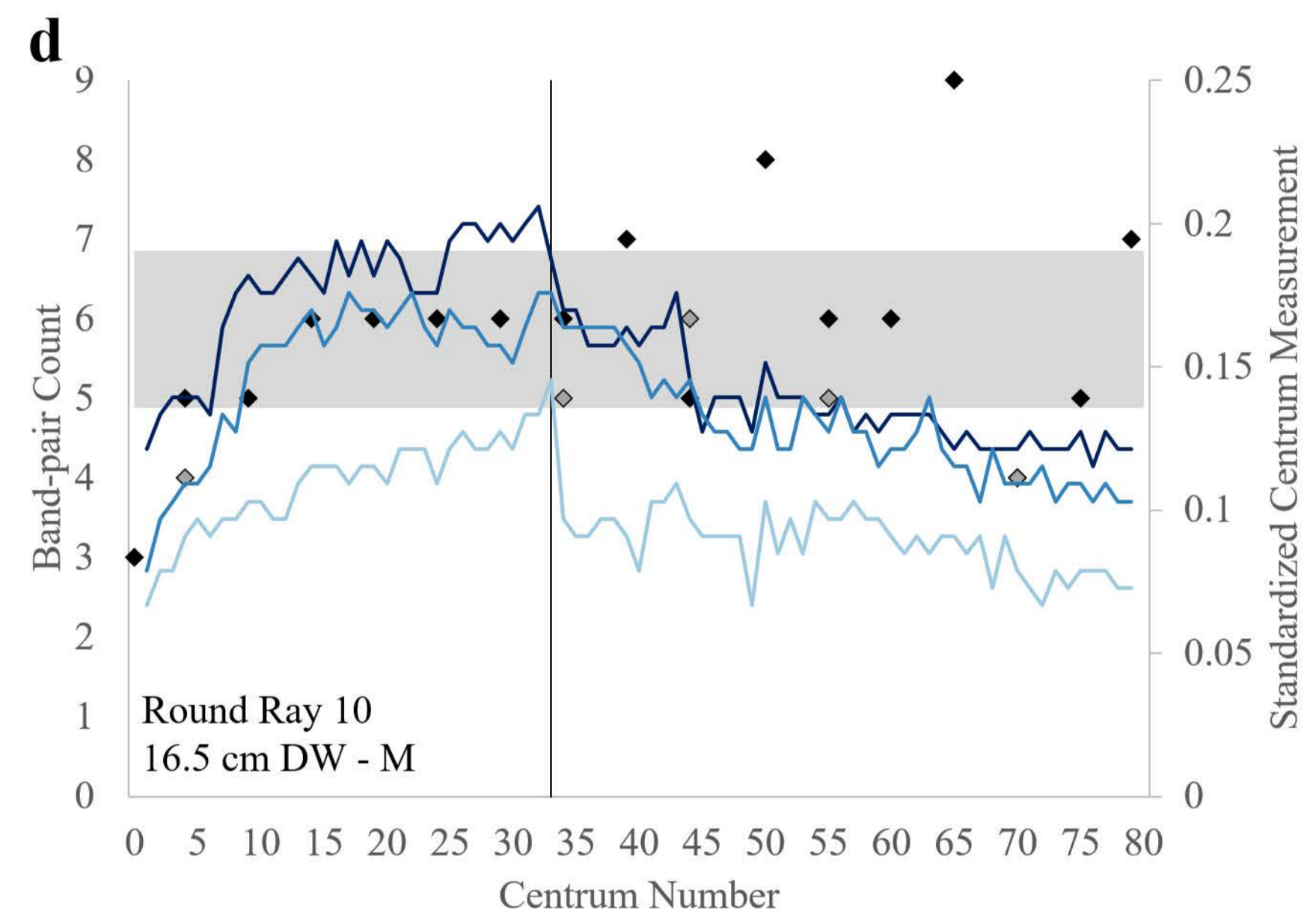
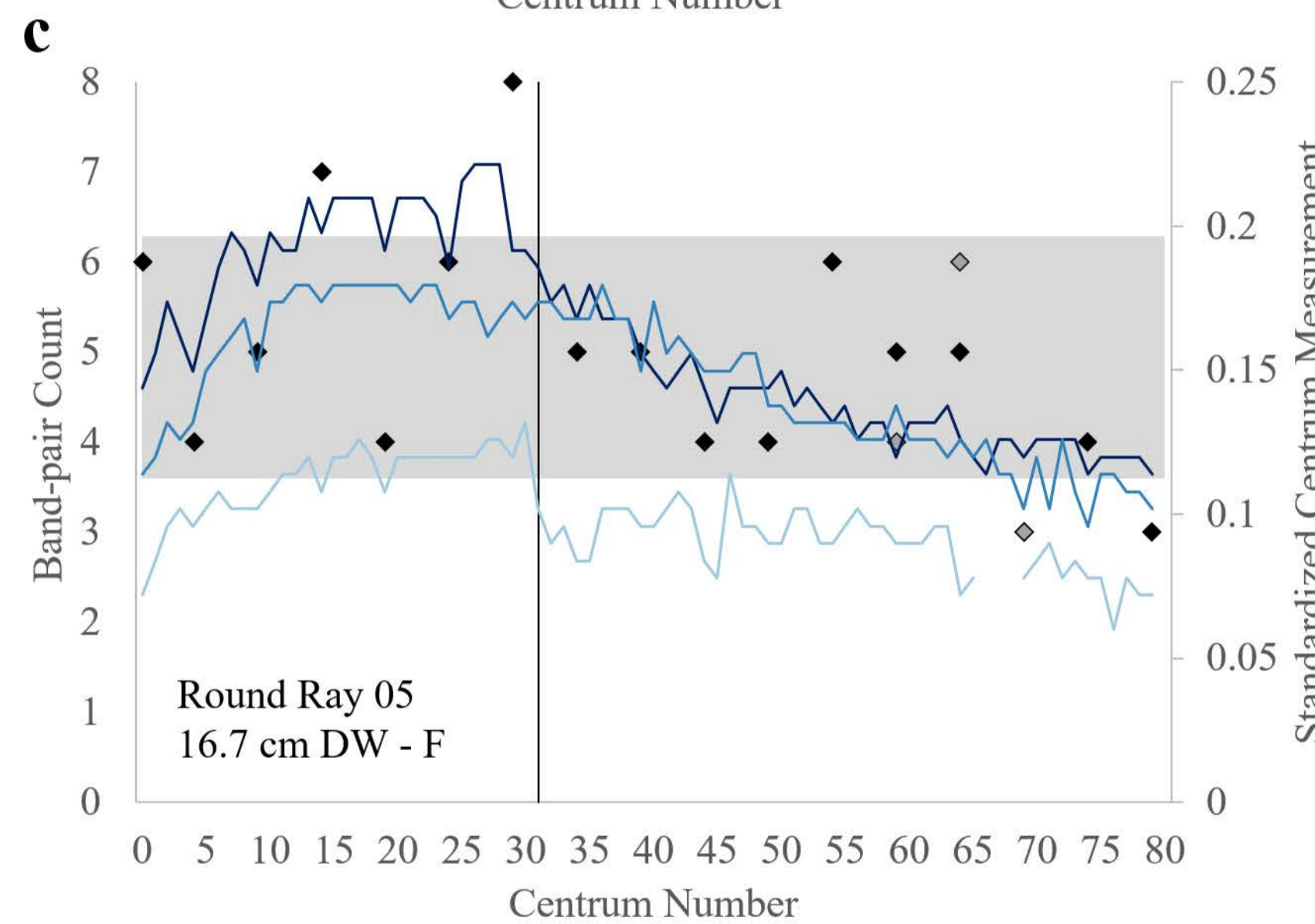
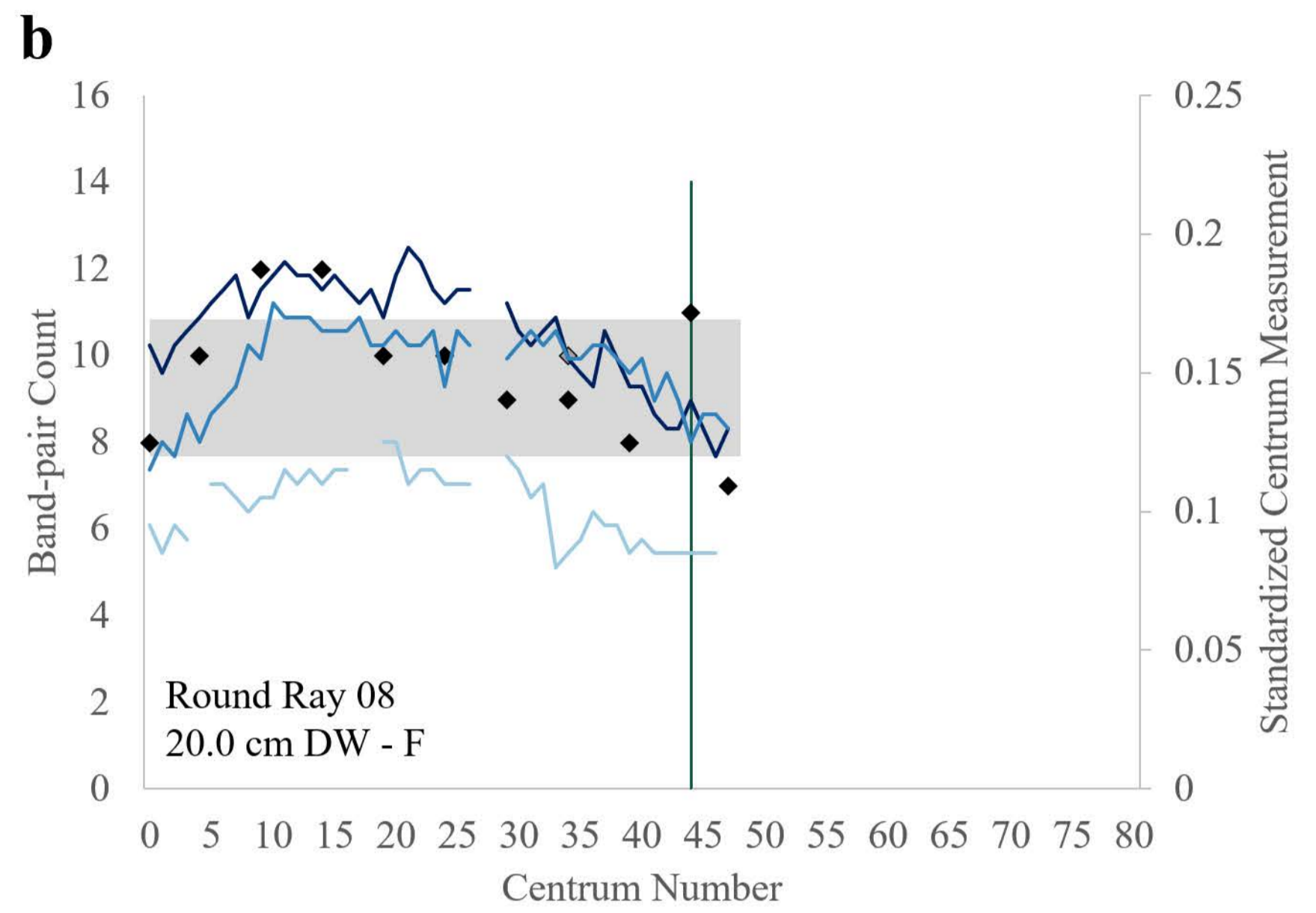
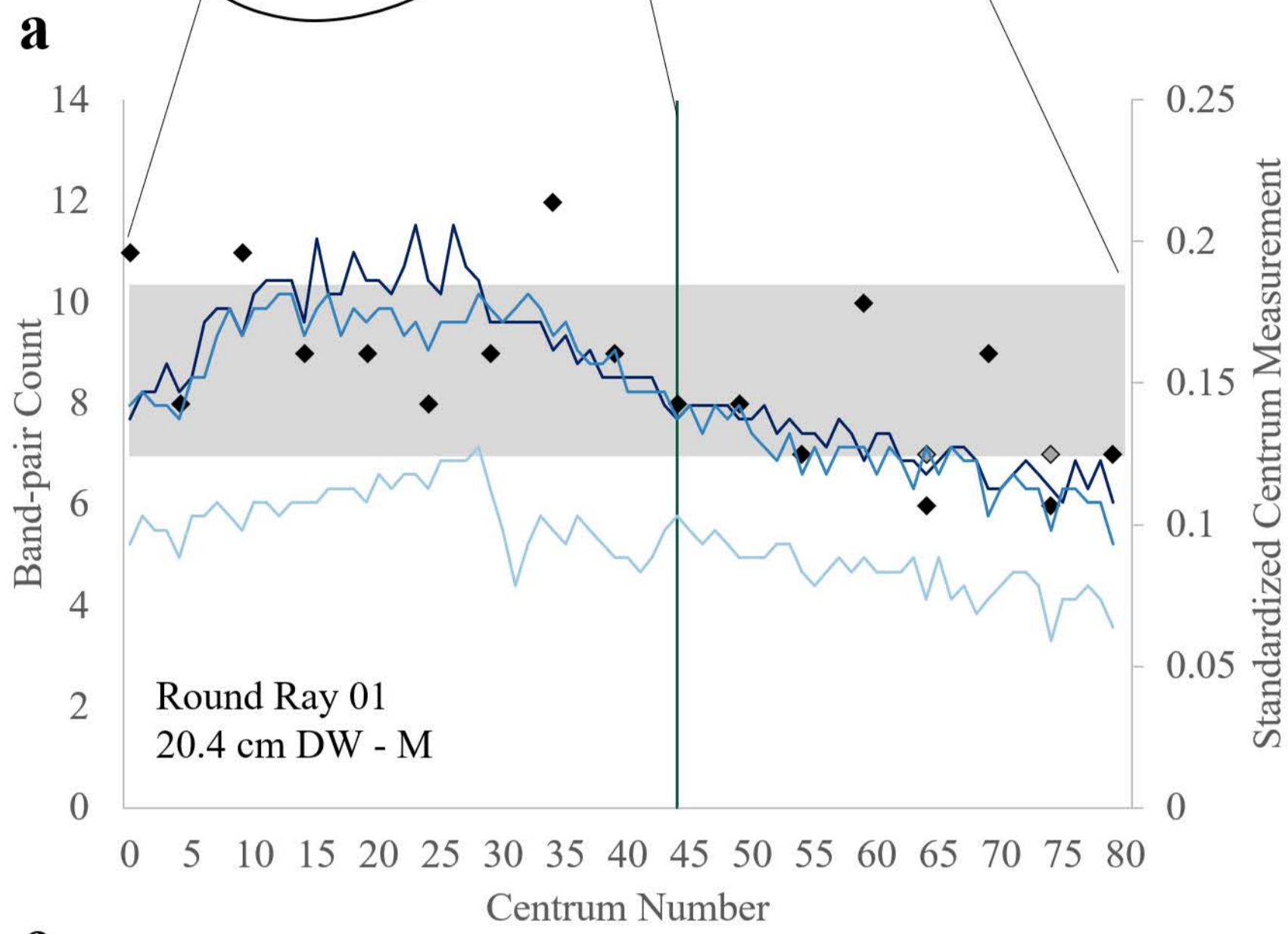




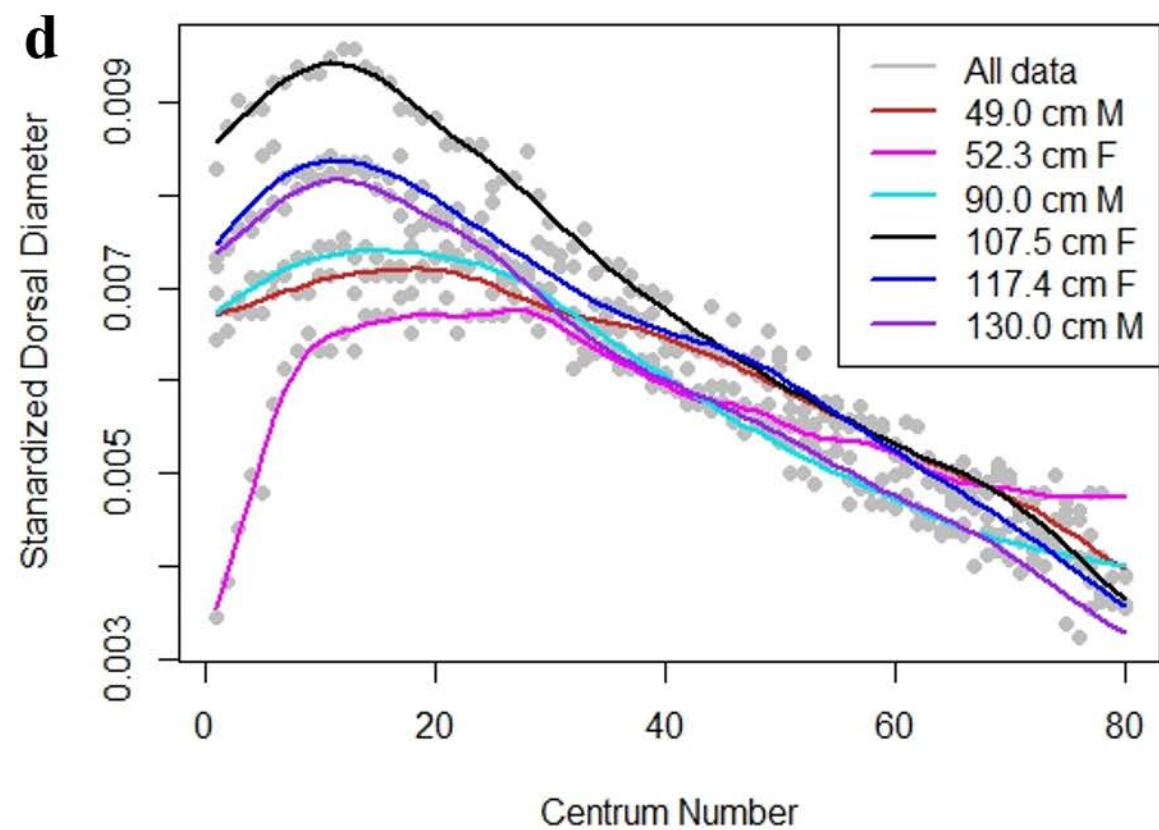
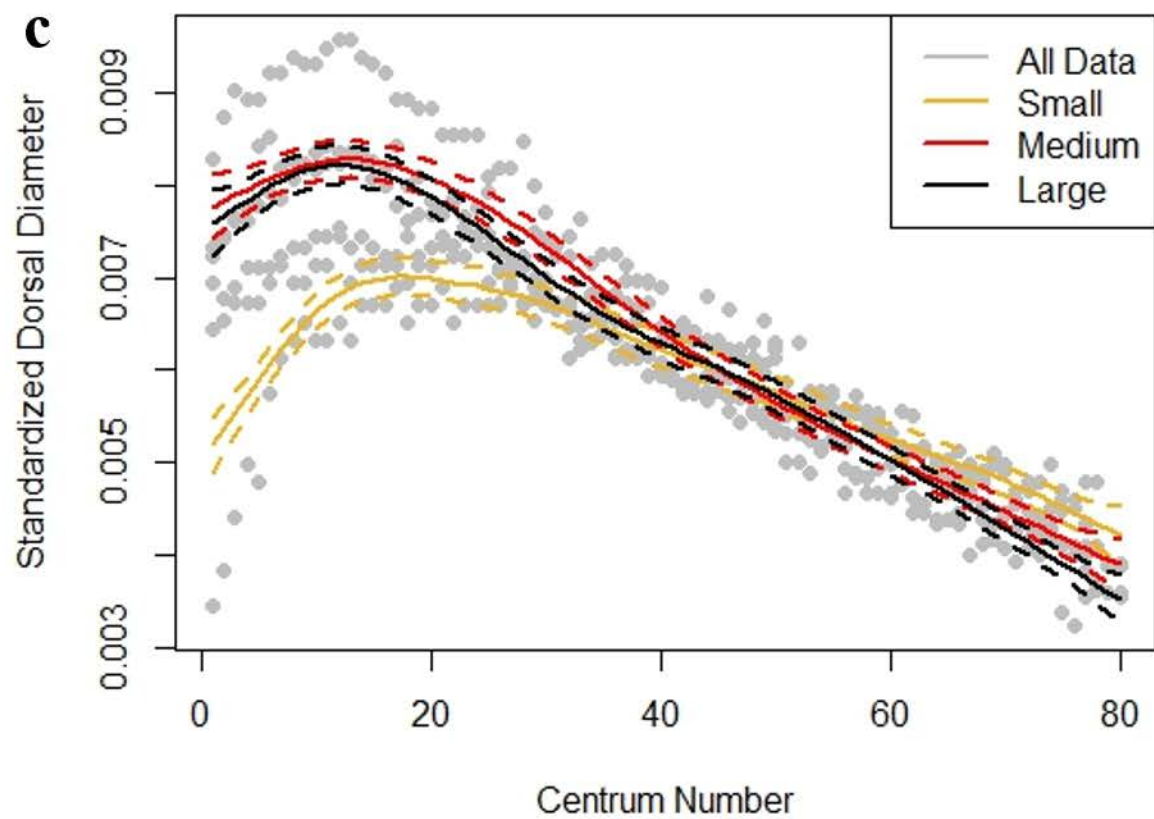
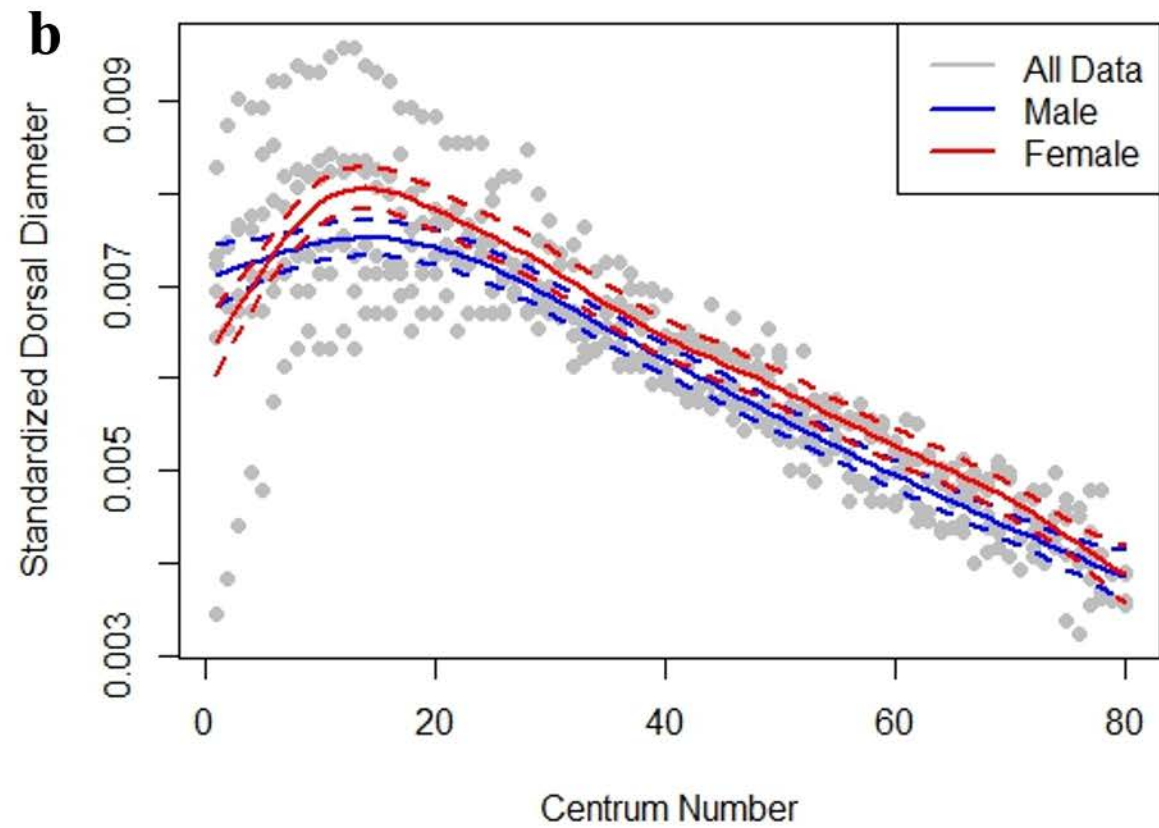
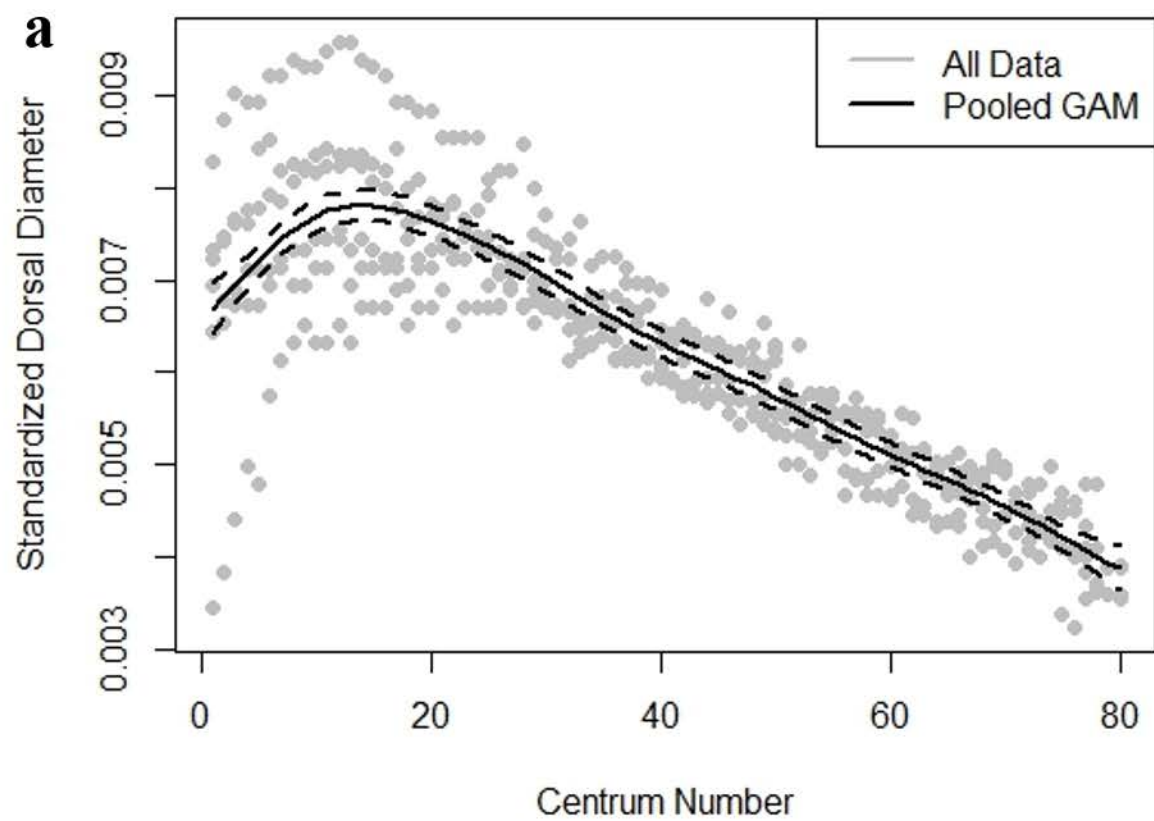


## Legend

- 95% Confidence Interval
- ◆ Primary Band-pair Count
- ◇ Consensus Band-pair Count
- End of Gut Cavity
- Standardized Lateral Diameter
- Standardized Dorsal Diameter
- Standardized Length









Supplementary Table 1. Generalized additive model results for 10 different models to best describe centrum morphology along the vertebral column for five batoid species. k is the number of knots used in each model.

Species	Model	Dorso-ventral Diameter				Lateral Diameter				Rostro-caudal Length							
		Deviance	k	Adjusted r <sup>2</sup>	AIC	AAIC	Deviance	k	Adjusted r <sup>2</sup>	AIC	AAIC	Deviance	k	Adjusted r <sup>2</sup>	AIC	AAIC	
Little Skate	Pooled	3277.71	15	0.84	-25275.12	4449.48	3273.56	18	0.88	-23443.01	4433.9	3088.55	15	0.45	-23522.05	2241.74	
	BySex	Different Smoother	3265.75	18	0.84	-25263.06	4461.54	3261.56	18	0.88	-23453.14	4423.8	3072.59	18	0.47	-23590.06	2173.73
		Different Intercept	3275.28	18	0.84	-25276.17	4448.43	3272.56	18	0.88	-23443.65	4433.3	3085.32	18	0.46	-23576.90	2186.89
		Different Smoother and Intercept	3264.76	18	0.84	-25261.29	4463.31	3260.57	18	0.88	-23454.93	4422	3071.55	18	0.48	-23637.57	2126.22
	BySize	Different Smoother	3256.68	18	0.85	-25330.62	4393.98	3250.89	18	0.89	-23733.30	4143.6	3060.25	18	0.52	-23877.46	1886.33
		Different Intercept	3274.29	18	0.84	-25278.37	4446.23	3271.6	18	0.88	-23440.82	4436.1	3084.36	18	0.47	-23575.90	2187.89
		Different Smoother and Intercept	3254.69	18	0.85	-25329.92	4394.68	3248.95	18	0.89	-23734.11	4142.8	3058.12	18	0.53	-23926.75	1837.04
	ByIndividual	Different Smoother	3034.36	18	0.9	-26446.93	3277.67	2963.43	18	0.93	-24876.66	3000.3	2756.94	18	0.65	-24496.00	1267.79
		Different Intercept	3234.89	18	0.9	-26696.52	3028.08	3232.78	18	0.92	-24667.08	3209.9	3045.69	18	0.58	-24288.32	1475.47
		Different Smoother and Intercept	2901.33	18	0.96	-29724.60	0	2813.94	18	0.97	-27876.94	0	2644.62	18	0.78	-25763.79	0
	Winter Skate	Pooled	462.05	15	0.86	-3614.77	926.251	462.03	16	0.86	-3451.75	691.53	454.63	13	0.52	-3589.57	414.821
		BySex	Different Smoother	452.01	18	0.87	-3650.95	890.077	451.25	18	0.88	-3489.35	653.93	449.49	10	0.54	-3602.86
Different Intercept			459.59	20	0.87	-3663.15	877.869	460.36	18	0.86	-3449.98	693.3	450.41	18	0.86	-3372.12	632.271
Different Smoother and Intercept			450.31	18	0.89	-3708.53	832.493	450.26	18	0.88	-3487.91	655.37	440.36	18	0.88	-3408.80	595.59
BySize		Different Smoother	443.47	15	0.93	-3896.50	644.521	439.29	17	0.92	-3677.35	465.93	441.87	10	0.58	-3633.88	370.514
		Different Intercept	459.99	16	0.87	-3638.81	902.213	459.56	17	0.88	-3481.86	661.42	451.96	14	0.6	-3677.31	327.083
		Different Smoother and Intercept	442.44	14	0.93	-3925.36	615.662	434.22	20	0.93	-3724.76	418.52	439.14	10	0.66	-3735.08	269.31
ByIndividual		Different Smoother	412.76	17	0.95	-4084.52	456.506	397.4	20	0.96	-3999.54	143.74	426.11	12	0.65	-3696.49	307.90
		Different Intercept	456.29	17	0.89	-3701.02	840.003	456.59	17	0.88	-3479.35	663.93	451.37	10	0.64	-3717.61	286.781
		Different Smoother and Intercept	378.1	23	0.98	-4541.02	0	385	20	0.97	-4143.28	0	394.28	17	0.83	-4004.39	0
Barndoor Skate		Pooled	459.00	10	0.79	-5574.04	1085.87	462.9	15	0.83	-5725.93	670.57	442.45	10	0.32	-5212.10	561.733
		BySex	Different Smoother	453.69	18	0.79	-5574.10	1085.81	458.24	10	0.83	-5731.21	665.29	437.25	10	0.33	-5209.29
	Different Intercept		457.93	10	0.8	-5594.87	1065.04	462.8	10	0.83	-5723.23	673.28	441.47	10	0.32	-5211.42	562.41
	Different Smoother and Intercept		453.24	10	0.8	-5596.25	1063.66	457.26	10	0.83	-5730.57	665.94	436.28	10	0.33	-5208.82	565.017
	BySize	Different Smoother	448.64	10	0.87	-5799.38	860.529	452.42	10	0.87	-5840.35	556.15	432.06	10	0.47	-5319.94	453.889
		Different Intercept	457.05	10	0.82	-5632.87	1027.04	461.75	15	0.86	-5808.95	587.56	440.27	10	0.4	-5263.24	510.597
		Different Smoother and Intercept	446.04	10	0.89	-5852.63	807.275	449.73	10	0.89	-5922.32	474.19	429.11	10	0.55	-5389.19	384.644
	ByIndividual	Different Smoother	433.82	10	0.92	-5955.65	704.26	434.07	10	0.93	-6090.14	306.37	418.69	10	0.52	-5348.10	425.73
		Different Intercept	453.72	10	0.89	-5807.76	852.147	457.46	10	0.89	-5875.56	520.94	437	10	0.57	-5417.61	356.227
		Different Smoother and Intercept	406.41	18	0.98	-6659.91	0	416.74	15	0.96	-6396.50	0	388.06	18	0.82	-5773.83	0
	Atlantic Stingray	Pooled	695.09	10	0.59	-4384.39	950.027	694.26	15	0.69	-4296.73	606.96	676.88	10	0.29	-4428.66	255.101
		BySex	Different Smoother	691.18	15	0.61	-4420.81	913.605	690.54	10	0.69	-4295.07	608.62	673.52	10	0.69	-4193.63
Different Intercept			693.28	15	0.59	-4382.33	952.085	694.03	10	0.69	-4307.25	596.44	677.05	10	0.69	-4206.18	477.585
Different Smoother and Intercept			690.2	15	0.61	-4418.96	915.457	689.51	10	0.69	-4307.12	596.57	672.5	10	0.69	-4206.19	477.577
BySize		Different Smoother	681.98	15	0.64	-4465.12	869.296	683.35	10	0.72	-4375.49	528.2	666.12	15	0.3	-4414.27	269.488
		Different Intercept	691.94	15	0.68	-4538.10	796.308	692.29	10	0.69	-4304.36	599.33	670.6	18	0.47	-4620.88	62.883
		Different Smoother and Intercept	678.48	15	0.72	-4634.37	700.044	681.32	10	0.73	-4379.01	524.68	660.07	15	0.46	-4587.61	96.157
ByIndividual		Different Smoother	658.12	10	0.66	-4487.95	846.458	654.97	10	0.74	-4386.82	516.87	648.52	10	0.28	-4378.91	304.85
		Different Intercept	686.68	10	0.81	-4891.77	442.645	686.89	15	0.82	-4661.20	242.49	665.7	15	0.52	-4683.76	0
		Different Smoother and Intercept	622.79	15	0.91	-5334.41	0	631	15	0.88	-4903.69	0	629.71	15	0.52	-4620.90	62.858
Round Ray		Pooled	750.84	16	0.81	-4794.71	538.898	751.51	15	0.84	-4662.83	468.25	743.36	15	0.66	-4860.46	236.788
		BySex	Different Smoother	745.95	10	0.81	-4806.81	526.799	742.96	15	0.85	-4710.33	420.76	736.55	15	0.67	-4891.93
	Different Intercept		752.88	10	0.82	-4831.30	502.313	749.58	18	0.85	-4680.77	450.32	742.35	15	0.66	-4869.58	227.665
	Different Smoother and Intercept		744.91	10	0.82	-4843.31	490.301	741.88	15	0.86	-4732.16	398.92	735.51	15	0.68	-4904.28	192.967
	BySize	Different Smoother	734.47	15	0.82	-4824.02	509.591	736.98	15	0.85	-4685.57	445.52	730.4	15	0.66	-4853.07	244.178
		Different Intercept	749.22	15	0.81	-4808.90	524.709	749.47	15	0.85	-4698.94	432.14	741.32	15	0.67	-4888.59	208.66
		Different Smoother and Intercept	732.75	14	0.82	-4841.70	491.916	738.3	10	0.86	-4720.63	410.46	728.5	15	0.67	-4880.24	217.012
	ByIndividual	Different Smoother	685.33	17	0.86	-4924.13	409.486	698.01	11	0.87	-4763.74	367.35	695.76	15	0.7	-4904.17	193.08
		Different Intercept	741.4	16	0.87	-5037.33	296.281	742.03	15	0.89	-4937.57	193.52	733.99	15	0.72	-5009.08	88.165
		Different Smoother and Intercept	656.47	23	0.92	-5333.61	0	680.26	12	0.92	-5131.09	0	681.04	15	0.77	-5097.25	0